Australian Government
Geoscience Australia

FOR PUBLIC RELEASE

Professional Opinion

No. 2010/05

The age of the Telfer Au-Cu deposit and its relationship with granite emplacement, Paterson Province, Western Australia

David W. Maidment, David L. Huston and Larry Heaman

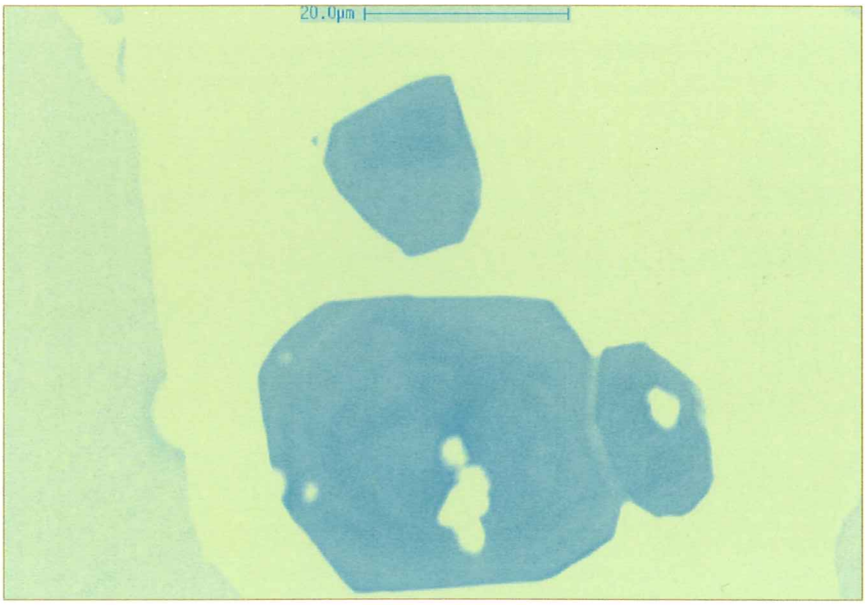

APPLYING GEOSCIENCE TO AUSTRALIA'S MOST IMPORTANT CHALLENGES

The age of the Telfer Au-Cu deposit and its relationship with granite emplacement, Paterson Province, Western Australia

GEOSCIENCE AUSTRALIA
PROFESSIONAL OPINION 2010/05

by

David W. Maidment[1], David L. Huston[1] and Larry Heaman[2]

Australian Government
Geoscience Australia

1. Geoscience Australia, GPO Box 378, Canberra, ACT 2601
2. Universitty of Alberta, Canada

Department of Resources, Energy and Tourism
Minister for Industry: The Honourable Martin Ferguson, AM MP
Secretary: Mr John Pierce

Geoscience Australia
Acting Chief Executive Officer: Dr Chris Pigram

GeoCat # 70102

Bibliographic reference: Maidment, D.W., Huston, D.L. and Heaman, L., 2010. The age of the Telfer Au-Cu deposit and its relationship with granite emplacement, Paterson Province, Western Australia. Geoscience Australia Profession Opinion 2010/05, 36pp.

Contents

Executive Summary

Dating of granites from the Telfer Region of the Paterson Province shows that felsic magmatism took place between ca. 645 Ma and ca. 605 Ma, with clusters at ca. 645, and ca. 630 and a single granite at 605 Ma (the O'Callaghans Granite). This magmatism is interpreted to be a result of deformation and crustal thickening associated with the Miles Orogeny, the first major compressional deformation to affect the Neoproterozoic sedimentary rocks of the Yeneena Basin. SHRIMP and ID-TIMS U-Pb dating of monazite and xenotime from Au-bearing veins at the Telfer Mine show that early concordant vein mineralisation took place at 652 ± 7 Ma, while a late-stage discordant vein yielded an age of 645 ± 7 Ma. These dates indicate that mineralisation took place over a relatively restricted period of time, at a similar time to the emplacement of the earliest granites of the Miles Orogeny, and was apparently unrelated to magmatism at ca. 630 Ma and ca. 605 Ma. Although there is a close temporal relationship between the early granites and Au mineralisation, the lack of a close spatial association suggests that it is possible that granite emplacement was not directly involved in the mineralising system, but was instead a separate consequence of deformation associated with the Miles Orogeny. If this was the case, then other parts of the Yeneena Basin affected by the Miles Orogeny, but not intruded by granites, could be prospective for lode-Au mineralisation.

Introduction

The Telfer Au-Cu deposit in the Paterson Province of Western Australia (Fig. 1) is a world-class deposit, with a total resource of 19.5 Moz Au and 680 kt Cu as of June 2007 (www.newcrest.com.au; accesssed July, 2008). Despite more than 30 years of exploration, the Telfer deposit remains the only major gold deposit in the province. The deposit is hosted by sedimentary rocks of the Neoproterozoic Lamil Group, which forms the stratigraphically upper part of the Yeneena Supergroup (Fig. 2), which filled the Yeneena Basin. Copper and gold are hosted by veins and strockworks that are concordant in the upper parts of the mine, but crosscutting at depth. Hence, early genetic models for the formation of the Telfer mineralisation favoured syngenetic-exhalative processes (e.g. Tyrwhitt, 1979, 1985; Turner, 1982), but an epigenetic-replacement model for ore formation is currently accepted based on the recognition that mineralisation is commonly hosted in structurally-controlled sites (Goellnicht et al., 1989; Dimo, 1990; Goellnicht, 1992; Rowins et al., 1997; Howard et al., 2000).

Although an epigenetic origin for mineralisation is widely accepted, the role of granites in the mineral system is the subject of some debate. Goellnicht (1987, 1992) suggested that granites emplaced during the ~650 Ma Miles Orogeny provided a significant contribution to hydrothermal fluids generating mineralisation, in addition to providing a heat source to drive fluid flow. This contrasts with the interpretation of Rowins et al. (1997), who considered the source of sulphur and metals to be the Neoproterozoic sedimentary rocks that host the mineralisation, based on C, O, B, Pb and S isotopic data from the ore and alteration assemblages. In this model, granites were primarily a heat source driving fluid flow and leaching of the sedimentary succession, with ore formation taking place in structurally controlled sites, not necessarily close to the granite.

In this study, we present the results of a geochronological study constraining the ages of the regional granites and the timing of ore formation at Telfer, with the aim of determining the temporal relationship between mineralisation and magmatism. The timing of these events provides important constraints on any model for mineralisation in the Paterson Province.

Regional Geology

The Paterson Province in Western Australia consists of polydeformed and metamorphosed basement rocks of the Palaeoproterozoic Rudall Complex overlain by weakly metamorphosed sedimentary rocks of the Neoproterozoic Yeneena and northwestern Officer basins (Hickman and Bagas, 1999; Bagas, 2004; Grey et al., 2005; Czarnota et al., 2007; Maidment, 2007).

The Yeneena Basin consists the Lamil and Throssell Groups (Fig. 3), which are not exposed in contact, but are interpreted to represent transgressive and regressive cycles of a single supersequence (McIntyre et al., 2005; Czarnota et al., 2007). The maximum age of the Yeneena Basin succession is constrained by detrital U-Pb SHRIMP zircon ages of c. 980 Ma for the Coolbro Sandstone at the base of the Throssell Group, and 920–915 Ma for the Malu Formation, c. 845 Ma for the Puntapunta Formation and c. 960 Ma for the Wilki Formation in the Lamil Group (Bagas and Nelson, 2007; Maidment et al., 2007). Minimum ages are provided by mafic and intermediate intrusions with SHRIMP U-Pb zircon and baddeleyite ages of 837 ± 6 and 835 ± 4 Ma (Maidment et al., 2007) and 816 ± 6 Ma (Reed, 1996) that intrude units through the Yeneena Supergroup. An age of 858 ± 29 Ma, based on a Pb-Pb isochron from carbonate of the Isdell Formation (Throssell Group) and interpreted as a diagenetic age (R Maas and D Huston, unpub. data), is consistent with these constraints.

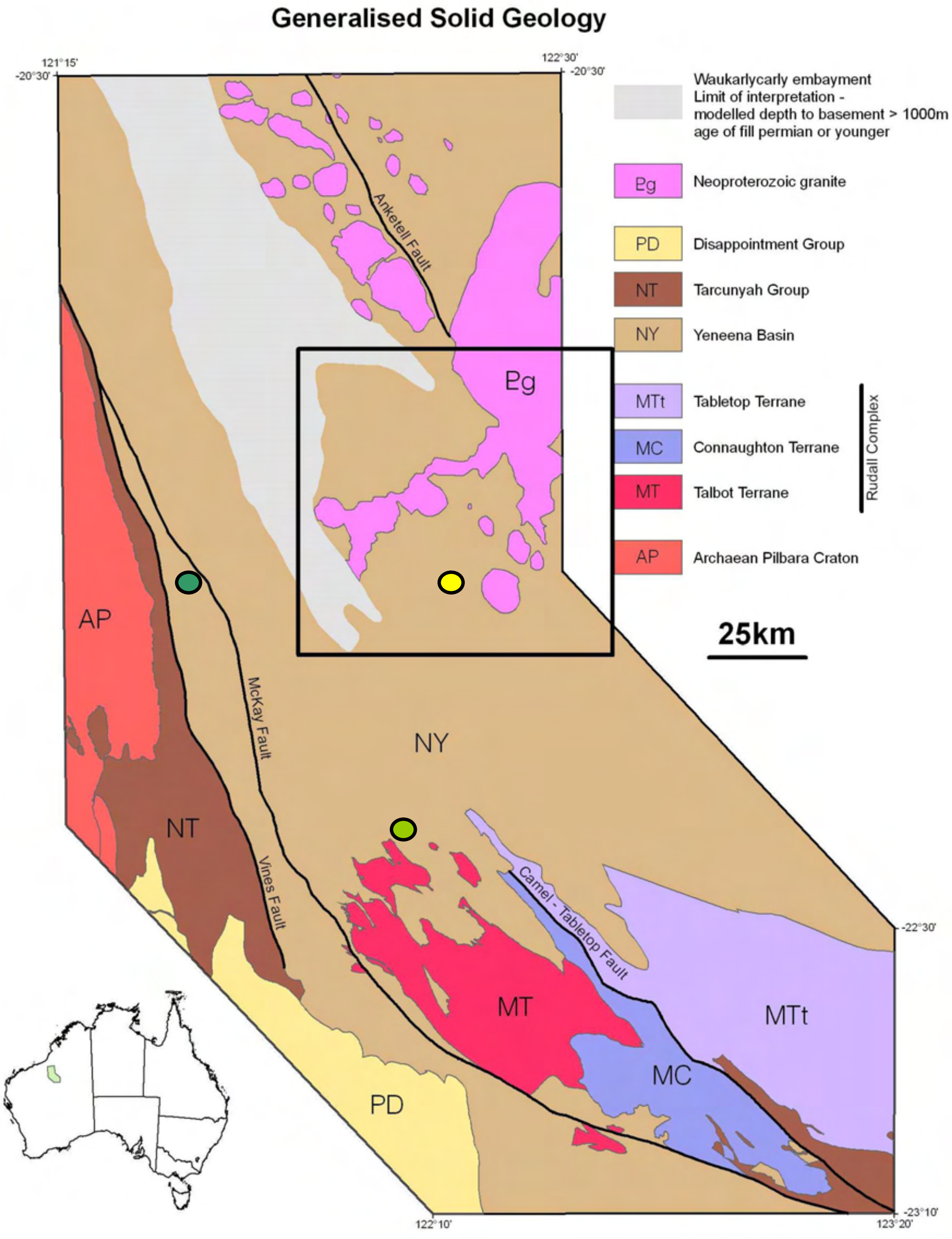

Fig. 1. *Regional geology of the Paterson Province. Closed circles show the locations of major deposits (yellow – Telfer; blue green – Nifty Cu; yellow green – Kintyre). Box indicates the location of Figure 3.*

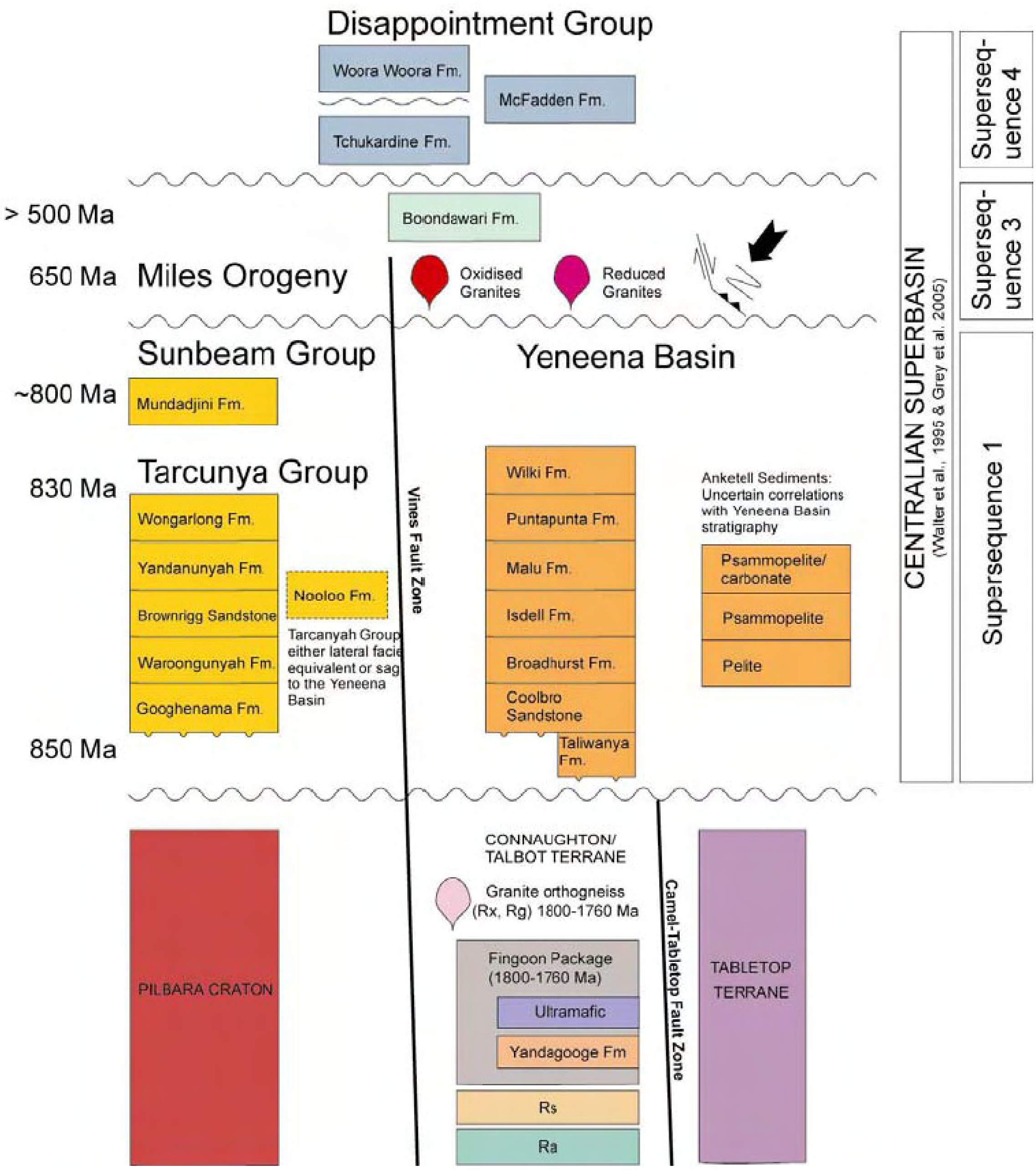

Fig. 2. *Stratigraphic relationships of the Paterson Province.*

The Miles Orogeny resulted in NW-trending folding and thrusting of the Yeneena Basin and Rudall Complex, and sub-greenschist to greenschist facies metamorphism in outcropping rocks (Bagas, 2004; Czarnota et al., 2007). Widespread intrusion of granites in the central and northern parts of the province is interpreted to be related to crustal thickening associated with the Miles Orogeny. In the Telfer area granites were emplaced along two approximately linear trends; the Crofton Trend which strikes northeast and the Wilki Trend which strikes roughly NNE (Fig. 3). The granites consist of highly fractionated, metaluminous, I-type monzogranites to K-feldspar granites, with some plutons having high concentrations of heat-producing elements (Goellnicht et al., 1991). The granites have a range of oxidation states, with the oxidised granites typically forming magnetic highs, while reduced granites form magnetic lows (Fig. 3). Goellnicht et al. (1991) divided the granites into two groups: (1) the weakly to strongly deformed Minyari group, consisting of less fractionated, ilmenite-series granites with 3-8 % biotite; and (2) the generally undeformed Mount Crofton group, consisting of more highly fractionated, magnetite-series granites with up to 2% biotite. Initial Pb isotopic compositions indicate that the Minyari and O'Callaghans granites of the Minyari Group might have had different source regions (Goellnicht et al., 1991), which led Budd et al. (2001) to classify the granites of the Paterson Province as the O'Callaghans Supersuite, as the plutons do not all meet the strict definition of the term 'suite' of White et al. (2001). Budd et al. (2001) argued that the classification of Goellnicht et al. (1991) should be revised as the main difference between the granites of the supersuite is the higher oxidation state of the Mount Crofton Granite compared with the other granites, and the differing initial Pb isotopic composition of the Minyari Granite. They considered that all the granites were likely to have been relatively oxidised at their source region, but that the earlier granites were reduced by interaction with reduced basinal brines.

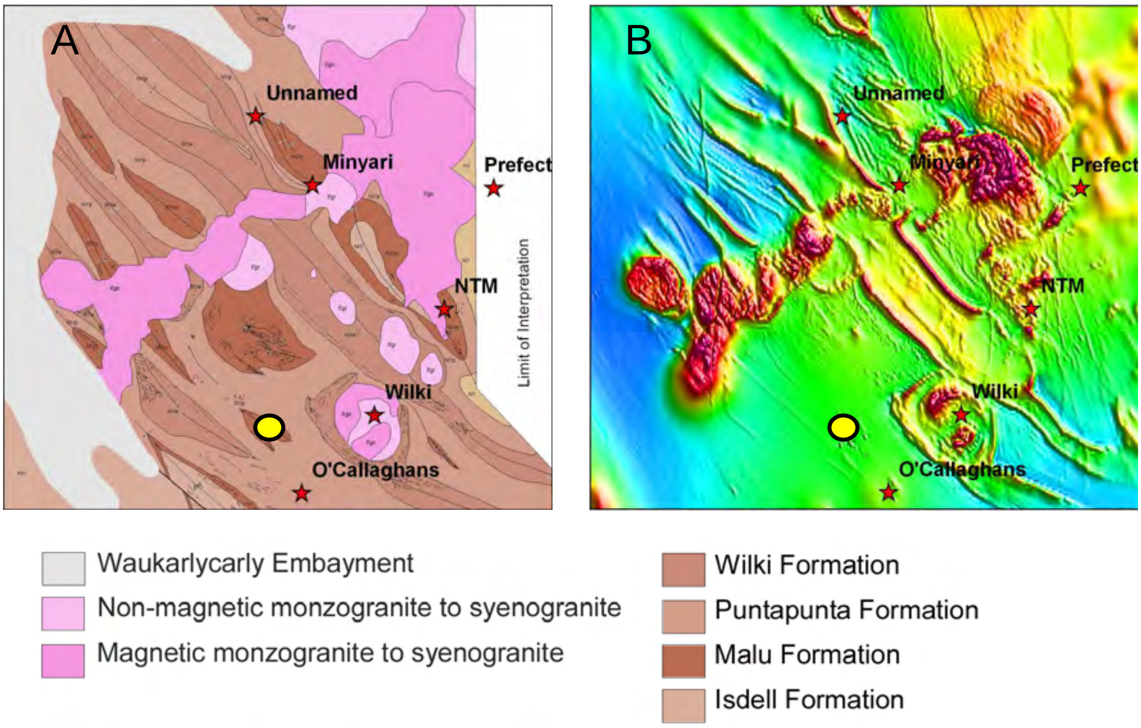

Fig. 3. *Location of geochronology samples (red stars) on (a) solid geology interpretation (Czarnota et al., 2009) (b) and total magnetic intensity image, reduced to pole. NTM refers to unnamed granite sampled by sample 2005671325. Unnamed refers to unnamed granite sampled by sample 2006671004. Yellow circle indicates the location of the Telfer deposit.*

Contact metamorphic aureoles around the granites range up to 2 km thick with metamorphic grades up to pyroxene-hornfels facies, to absent in the case of the O'Callaghans Granite (Chin et al., 1982; Goellnicht, 1992). Where present, the metamorphic aureoles commonly form magnetic highs, and delineate the boundaries of reduced granites (Czarnota et al., 2009).

There are no geochronological data that precisely date the age of the Miles Orogeny, with the best constraints being ^{40}Ar-^{39}Ar muscovite ages of 671-646 Ma obtained from the Rudall Complex and Coolbro Sandstone (Durocher et al., 2003). A minimum age for much of the deformation is provided by the SHRIMP U-Pb 654-640 Ma ages for the Mt Crofton Granite (Dunphy and McNaughton, 1998), which cross-cuts folding north of the Telfer mine (Fig. 3). Previous geochronology for the O'Callaghans Supersuite include a Rb-Sr whole rock age of 614 ± 42 Ma[1] (Trendall, 1974) and a Pb-Pb isochron age of 690 ± 48 Ma (McNaughton and Goellnicht, 1991) for the Mount Crofton Granite. More precise SHRIMP U-Pb ages have been obtained for zircon and titanite from the granites in the Telfer area by Dunphy and McNaughton (1998) who reported zircon ages of 629 ± 8 Ma and 621 ± 8 Ma for the Minyari Suite that were indistinguishable from a 633 ± 13 Ma zircon age obtained by Nelson (1995), and titanite ages that were slightly older (632 ± 5 and 645 ± 4 Ma). In the more fractionated Mount Crofton suite, a zircon age of 621 ± 13 Ma (Nelson, 1995) was also younger than titanite ages from the same suite, which yielded ages of 654 ± 8 and 640 ± 8 Ma (Dunphy and McNaughton, 1998). Dunphy and McNaughton (1998) considered the younger zircon ages to be a result of the high uranium content of the zircons, resulting in radiation damage to the crystals and lead loss. They thus considered the titanite ages to be the best estimate of the emplacement age of Mount Crofton suite.

Following the Miles Orogeny, the Paterson Orogeny resulted in relatively minor deformation of the Yeneena Basin and the Rudall Complex, with shortening oriented approximately NW-SE, orthogonal to that of the Miles Orogeny (Bagas, 2004). The timing of deformation remains poorly constrained, but is interpreted to have taken place at about 554 Ma, based on a ^{40}Ar-^{39}Ar feldspar age of 554 ± 7 Ma obtained from the Rudall Complex near the Kintyre deposit (Durocher et al., 2003). If this age is correct, then the Paterson Orogeny is broadly coincident with more intense transpressional deformation associated with the Petermann Orogeny in the Musgrave Inlier and strike-slip deformation in the Capricorn Orogen (Camacho et al., 1997; Sheppard et al., 2007).

MINERALISATION

The Paterson Province hosts three significant mineral deposits, the Telfer Au-Cu deposit, the Nifty Cu deposit and the Kintyre U deposit (Fig. 1). The Nifty Cu deposit is hosted by the Broadhurst Formation (Throssell Group), with a Sm-Nd isochron age for ore-related apatite indicating that the deposit formed at 791 ± 43 Ma, shortly after deposition of the host succession (Huston et al., 2007). The Cu mineralisation has a similar age to a uraninite ID-TIMS U-Pb age of c. 840 Ma obtained from unconformity-style U mineralisation at the Kintyre deposit within the Rudall Complex (Maas & Bagas, unpub. data; in Huston et al., 2009), suggesting that the Nifty Cu mineralisation could be part of a larger-scale, multi-element mineral system that has similarities to sediment-hosted mineralisation in the Zambian Copper Belt (Huston et al., 2007, 2009; Maidment et al., 2007). The Telfer Au-Cu deposit apparently post-dates the Nifty-Kintyre mineralisation, and is interpreted to be related to deformation and granite emplacement during the Miles Orogeny, though there are no publicly available ages for mineralisation to confirm this interpretation.

[1] Unless otherwise noted, cited uncertainties for previously published isochron and pooled ages are 2σ.

Geology of the Telfer deposit

The Telfer deposit occurs primarily within the Malu Formation, which consists of interbedded sandstone and siltstone and is exposed in the core of the Telfer Dome, a doubly-plunging anticline that comprises part of a larger NW-trending anticlinal structure interpreted to have formed during the ~650 Ma Miles Orogeny (Fig. 4). The mineralisation occurs as early vertically stacked quartz-pyrite concordant reef systems (the E-reefs, Middle Vale Reef, M-Reefs, A-Reefs, B-Reefs), which are cross-cut by quartz-dolomite-pyrite-gold veins, breccia zones and stockwork veins.

Early workers favoured a syngenetic model for mineralisation (Tyrwhitt, 1979, 1985; Turner, 1982), but as deeper levels of the deposit were exposed, it became evident that mineralisation was predominantly hosted in structurally controlled sites (Goellnicht et al., 1989; Dimo, 1990; Goellnicht, 1992; Rowins et al., 1997; Howard et al., 2000, 2005). The concordant reef systems are localised within interbedded siltstone and sandstone and are interpreted to have formed by bedding-plane slip along sites of contrasting rheology during deformation associated with the Miles Orogeny (e.g. Goellnicht et al., 1989; Howard et al., 2005). The discordant mineralisation is localised within relatively thick competent sandstone units that accommodated strain by brittle fracturing (e.g. Howard et al., 2005).

The main styles of reef and vein mineralisation and their relative timings are listed below:

1. Early quartz reefs – quartz and minor sulphides
2. Early stockwork veins – grey dolomite, quartz, albite ± muscovite, epidote, sericite and minor sulphides.
3. Discordant North-Dipping Veins (NDVs) – pink dolomite, calcite, quartz, chlorite, muscovite, pyrite, chalcopyrite ± scheelite and tourmaline.
4. Discordant Northwest-striking Veins (NWVs), conjugate veins and thrusts – quartz ± disseminated sulphide, scheelite, tourmaline, calcite and chlorite.
5. Late sulphide veins – galena ± disseminated sulphides.

Note that the orientation of the veins noted in the mine terminology as listed above, reflects the orientation of the veins relative to the local mine grid (Fig. 4).

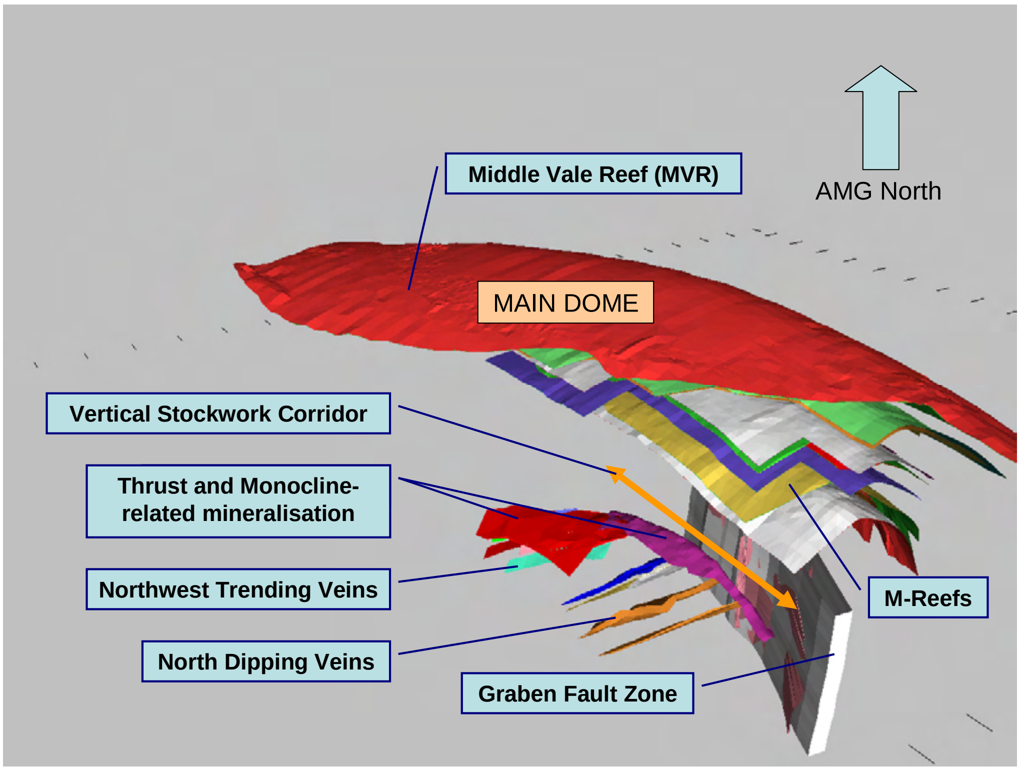

Fig. 4. *Schematic representation of the main phases of mineralised vein development within the Telfer Main Dome. Isometric view looking northwest (magnetic north). 200 m grid spacing.*

The broad spatial association between granites and mineralisation has led to the inference that Au mineralisation was related to granite emplacement, presumably occurring towards the end of the Miles Orogeny as the main granite trends cross-cut the NW-trending structural grain (Fig. 3). Goellnicht et al. (1989) noted that fluid inclusions from quartz veins were indicative of mixing of hot, very high salinity magmatic fluids with cooler, lower salinity basinal or meteoric waters, with Pb isotope sulphide data indicating that Pb was derived from the host rocks with a minor magmatic component. Rowins et al. (1997) challenged the interpretation that magmatic fluids were a significant input to the mineralising fluids at Telfer. Instead, they presented carbon, oxygen, boron, lead and sulphur isotope data that suggest ore solutes were derived from the sedimentary host rocks rather than the Neoproterozoic granites. They proposed a model in which the granites main role was as a heat source, driving fluid flow and scavenging of metals and sulphur from the Neoproterozoic sedimentary succession.

Methodology

Granites of the O'Callaghans Supersuite were dated using zircon, with cathodoluminescence (CL) imaging used to avoid areas with high-U and radiation damage. Zircon concentrates were prepared from 3-15 kg rock samples using clean heavy liquid and magnetic mineral separation techniques. Hand picked zircon was mounted in epoxy resin with zircon standards SL13, QGNG and Temora 2. Mounts were documented prior to analysis by reflected and transmitted light photomicroscopy and CL imaging on a Hitachi S-2250N SEM at the ANU Electron Microscopy Unit. U-Th-Pb isotopic analyses were carried out on SHRIMP A and SHRIMP B at Curtin University using procedures similar to those described by Williams and Claesson (1987) and Claoué-Long et al. (1995). The diameter of the analysis spot was ~20-40 µm with primary ion currents of ~2-4 nA O_2-. Positive secondary ions were extracted at 10 kV, mass analysed at a resolution of ~5000 and the Zr, Pb, U and Th species of interest measured on a single electron multiplier by cyclic stepping of the magnetic field. Fractionation of Pb relative to U was corrected using the relationship $Pb^+/U^+=A(UO^+/U^+)^2$ (Claoué-Long et al., 1995). The compositions assumed for standards were SL13: U = 238 ppm; Temora 2: radiogenic $^{206}Pb/^{238}U$ = 0.06683; QGNG: radiogenic $^{206}Pb/^{238}U$ = 0.33076. Ages were calculated using the decay constants recommended by the IUGS Subcommission on Geochronology (Steiger and Jäger, 1977). Analytical uncertainties listed in tables and plotted in figures are one standard error precision estimates. Uncertainties in pooled ages are 95% confidence limits and include the uncertainty in the Pb/U analysis of the standard.

Monazite and xenotime concentrates from mineralised veins at the Telfer deposit were prepared using clean heavy liquid and magnetic mineral separation techniques. Five hand picked fractions, each consisting of five grains, were prepared for each sample and submitted for thermal ionisation mass spectrometry (TIMS) analysis at the University of Alberta. Titanite extracted from the O'Callaghans Granite was prepared as five fractions, each consisting of 30 grains, and sent to the University of Alberta for analysis. Following washing in 4N HNO_3 for one hour at 70°C and loading into screw-top PFA Teflin vessels, all aliquots, together with a ^{205}Pb-^{235}U spike, were dissolved on a hot plate for 60 hours at a temperature of 80°C. Monazite and xenotime separates were dissolved in 6N HCl, whereas the titanite separates were dissolved in a 15:1 HF:HNO_3 mixture. After checking for complete dissolution, the aliquots were evaporated to dryness and then converted to chloride form in an oven at 215°C for 10-16 hours. Uranium and lead were purified using ion exchange chromatography. The purified uranium and lead aliquots were loaded together with 20 µL silica gel and 35 µL 1.5 N H_3PO_4 onto outgassed rhenium filaments. Analyses were preformed in a VG354 thermal ionisation mass spectrometer. More details of the analytical procedures are presented by Heaman et al. (2002). Sample locations are shown in Figure 2. Grid references are reported using the GDA94 datum in UTM coordinates, Zone 51.

Granite geochronology

Six granites were sampled to constrain the range of ages in the O'Callaghans Supersuite and to provide a reference against which the age of Telfer mineralisation could be compared. Samples were obtained from both the Crofton and Wilki trends and include both oxidised and reduced variants. Zircons obtained from the Mount Crofton Granite have extremely high U contents and could not be dated. All SHRIMP analyses are presented in Appendix A.

MINYARI GRANITE, GA SAMPLE 2006671025 (424144E, 7633932N)

The Minyari Granite forms a magnetic low within the Crofton Trend, cross-cutting NW-trending folding formed during the Miles Event (Fig. 3). A surface sample (with a magnetic susceptibility of 0.8×10^{-3} SI units) was sampled for dating, consisting of weakly altered, foliated, fine-grained biotite monzogranite. Biotite in the sample is commonly chloritised and locally altered to epidote. Feldspars are commonly dusted by sericite and carbonate and are also locally altered to epidote. Zircon from the granite is subhedral to euhedral with oscillatory zoning (Fig. 5a) and U contents ranging from 80-1100 ppm, with typical values of 100-500 ppm. Excluding one analysis of an inherited core with a discordant age of ~1285 Ma (M21.1) and a second analysis with high analytical uncertainty (M16.1), 18 zircon analyses form a cluster with a weighted mean $^{206}Pb/^{238}U$ age of 629.2 ± 3.0 Ma, with an acceptable MSWD of 0.63 (Fig. 6a).

WILKI GRANITE, GA SAMPLE 2005671291 (433321E, 7600012N)

The Wilki Granite is situated within the core of the complex Wilki Structure, about 15 km east of the Telfer Mine. Although poorly exposed, aeromagnetic data show the granite is comprised of differing phases of high and low magnetisation (Fig. 3). A sample of weakly magnetised granite was sampled from material excavated at the side of a track. This sample consists of unfoliated, medium-grained biotite monzogranite. Biotite is locally altered to chlorite, and albite and orthoclase are dusted by sericite. Zircons from the granite are comprised of relatively large euhedral crystals (to 150 μm) with oscillatory zoning (Fig. 5b) and moderate U contents of 170-740 ppm. One analysis of an inherited zircon core has an age of ~1050 Ma (W9.1), with analyses of oscillatory-zoned zircon yielding a $^{206}Pb/^{238}U$ age of 645.4 ± 3.8 Ma for a group of 19 analyses (MSWD = 1.2; Fig. 6b), excluding four slightly younger ages with high $f^{206}Pb$ (0.23-1.50%: W5.1, W6.1, W8.1 and W23.1), interpreted to have undergone a small amount of lead loss, and one analysis with high UO/U (W18.1: Appendix 1).

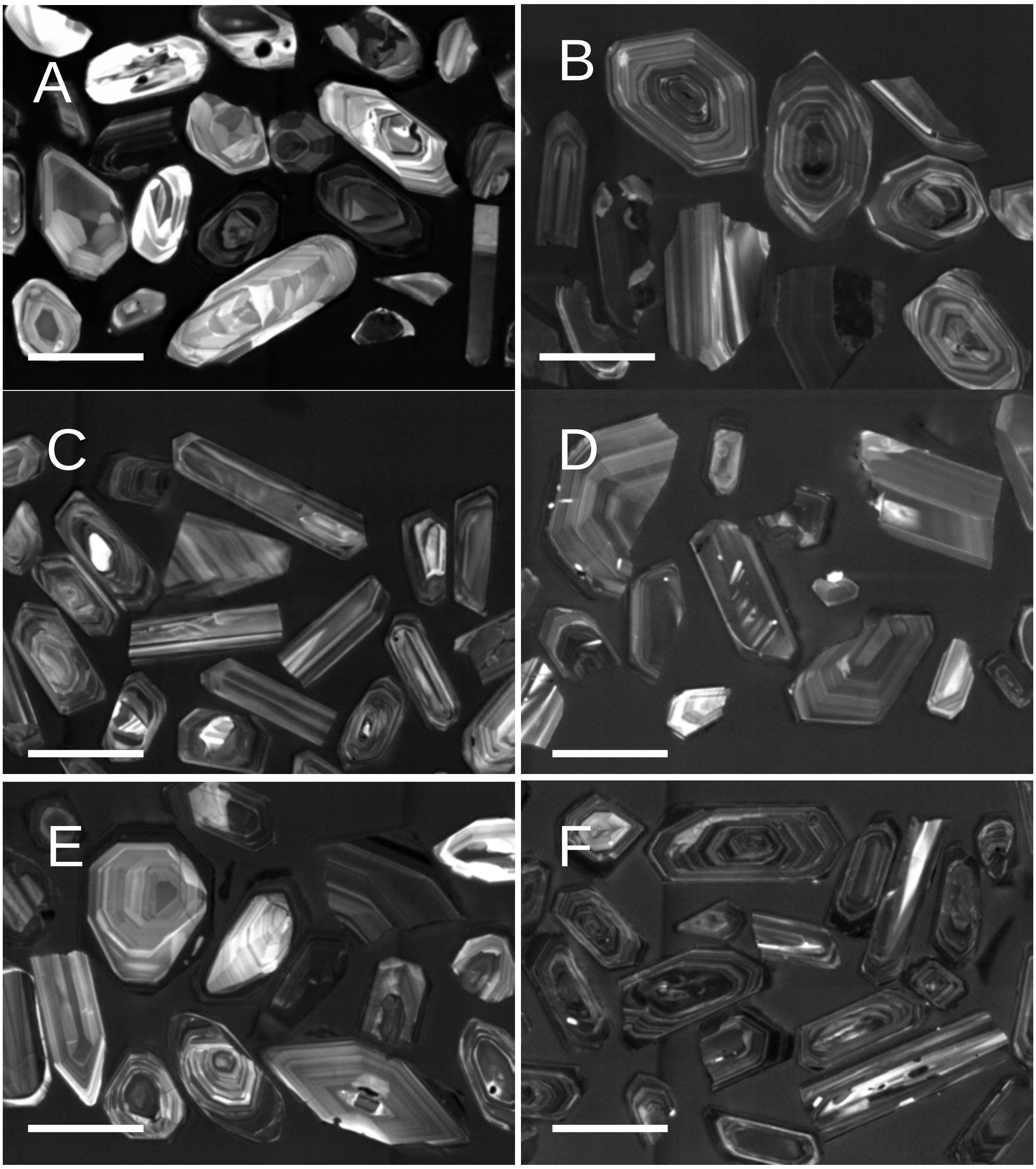

Fig. 5. *Cathodoluminescence images of zircons from the (a) Minyari Granite, (b) Wilki Granite, (c) unnamed granite near the Prefect prospect, (d) unnamed granite northwest of Minyari Hill, (e) unnamed granite east-northeast of Telfer, and (f) O'Callaghans Granite. The scale bars are 100 μm.*

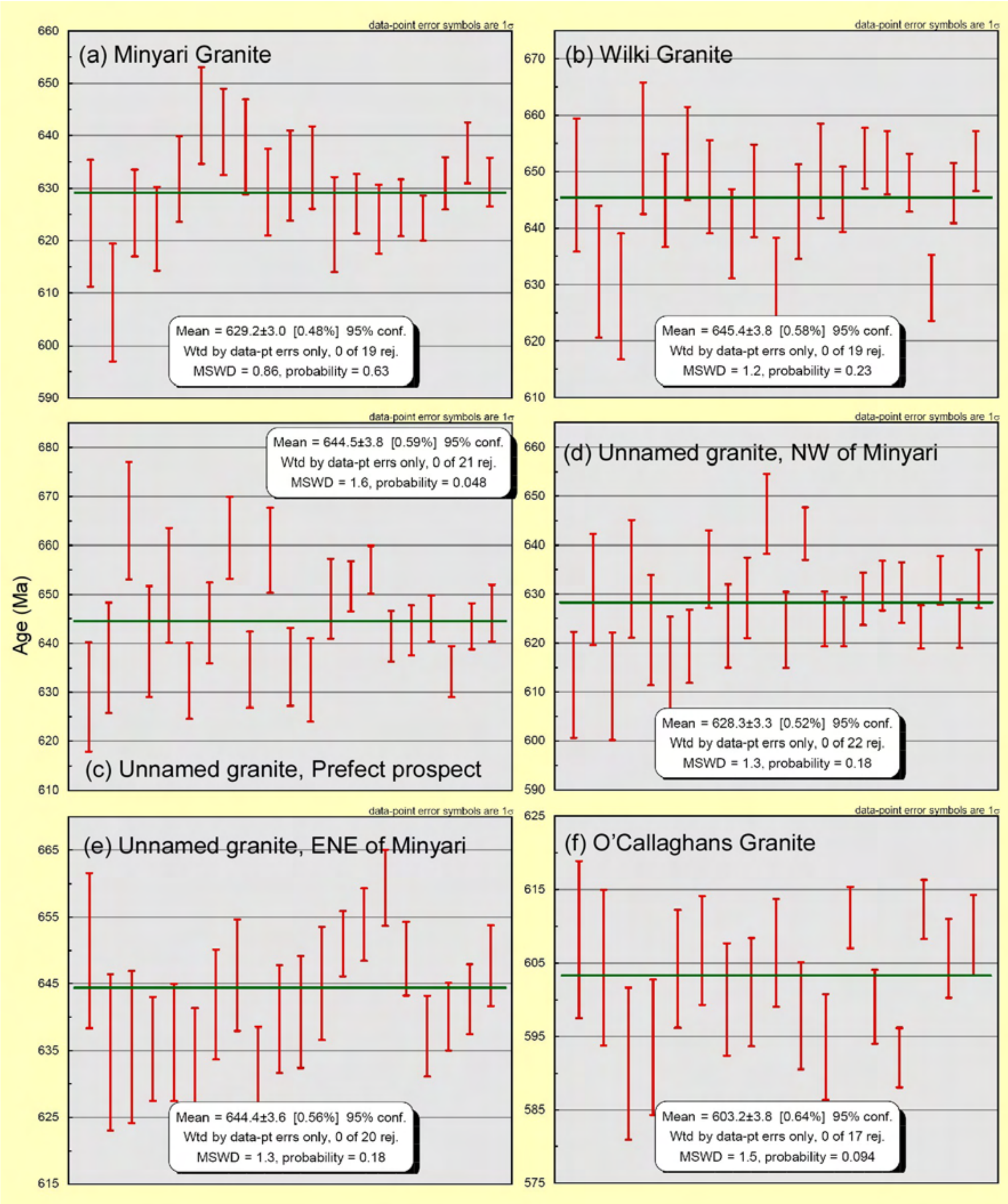

Fig. 6. *Diagrams showing weighted mean analyses from SHRIMP U-Pb zircon data from the (a) Minyari Granite, (b) Wilki Granite, (c) unnamed granite near the Prefect prospect, (d) unnamed granite northwest of Minyari Hill, (e) unnamed granite east-northeast of Telfer, and (f) O'Callaghans Granite.*

UNNAMED GRANITE, PREFECT PROSPECT, GA SAMPLE 2006677122 (450902E, 7633518N)

An unnamed, unexposed granite was sampled from drill core at the Prefect Prospect ~45 km northeast of the Telfer Mine (Fig. 3). The buried granite forms a magnetic high in airborne geophysical data, but the granite itself has a low magnetisation, and the high magnetic response is interpreted to be a result of a highly magnetised contact aureole. The sample consists of medium-to coarse-grained, unfoliated biotite monzogranite. Biotite is commonly chloritised, and feldspars are generally dusted by sericite. Zircon from the granite consists of oscillatory-zoned crystals with U contents of 175-727 ppm, which in some examples contain small, lower-U cores (Fig. 5c). Twenty-one analyses of the oscillatory-zoned zircon yield a weighted mean $^{206}Pb/^{238}U$ age of 644.5 ± 3.8 Ma, with an acceptable MSWD of 1.6 (Fig. 6c), excluding two analyses that overlapped inherited cores (P4.1 and P21.1) and one analysis (P25.1) that was not focussed during analysis.

UNNAMED GRANITE, NORTHWEST OF MINYARI, GA SAMPLE 2006671004 (415810E, 7644102N)

A sample of weakly magnetised granite was collected from a small outcrop exposure ~10 km northwest of Minyari Hill (Fig. 3). The sample consists of unfoliated, fine- to medium-grained biotite mozogranite. Biotite in the sample is commonly weakly chloritised and is locally altered to epidote, and feldspars are generally dusted by sericite. The sample contains euhedral, oscillatory-zoned zircon (Fig. 5d) with U contents of 128-1897 ppm (typically 200-600 ppm). Excluding one analysis (U8.1) with high $f^{206}Pb$ (1.7%), one analysis that experienced multiplier problems during analysis (U17.1) and one analysis with callibration problems (U14.1), 22 analyses form a cluster with a weighted mean $^{206}Pb/^{238}U$ age of 628.3 ± 3.3 Ma (MSWD = 1.3; Fig. 6d).

UNNAMED (NTM) GRANITE, EAST-NORTHEAST OF TELFER, GA SAMPLE 2005671325 (443603E, 7615675N)

An unnamed granite cropping out 25 km ENE of the Telfer Mine was sampled for geochronology. It consists of unfoliated, fine-grained hornblende monzogranite and has a low magnetic susceptibility, with magnetic contact aureoles in places (Fig. 3). The hornblende is commonly replaced by epidote, and minor carbonate replaces feldspar. This granite is unusual compared with other granites in the Paterson Province (e.g., Goellnicht et al., 1991) in having hornblende as the dominant, in this case, only ferro-magnesian mineral. Zircons from the granite are euhedral to subhedral, commonly with a low CL-brightness rim, and a few grains contain cores (Fig. 5e). Excluding two cores with ages of ~1580 (N5.1) and ~1315 Ma (N6.1) and two analyses collected during a period of instrument instability (N4.1 and N22.1), 20 zircon analyses form a cluster with a weighted mean $^{206}Pb/^{238}U$ age of 644.4 ± 3.6 Ma (MSWD = 1.3; Fig. 6e).

O'CALLAGHANS GRANITE, GA SAMPLE 2007670001 (422565E, 7588515N)

The O'Callaghans Granite is a reduced, low magnetisation buried intrusive that has been intersected in drilling at the O'Callaghans prospect ~10 km SSE of the Telfer Mine (Fig. 3). The granite consists of pink K-feldpsar, biotite and quartz that shows a well-defined foliation in places (Fig. 7). The sample collected for dating is strongly potassically altered fine- to medium-grained biotite syenogranite. Least altered domains in the sample consist of orthoclase and quartz with lesser albite and biotite and trace titanite and zircon. In these areas, orthoclase and, to a lesser extent, albite are extensively replaced by sericite.

The dominant alteration assemblage is pink in colour and consists of texturally destructive pervasive microcline replacement of primary granite, leaving relict orthoclase that is embayed and replaced by microcline. Accesory minerals associated with microcline include titanite and rutile. The microcline assemblage is veined by irregular and discontinuous quartz veins that also contain hydrothermal biotite, muscovite, carbonate, sulphide minerals and apatite. The dominant sulphide is pyrite, which is closely associated with carbonate. Molybdenite is also present, along with trace chalcopyrite and sphalerite. The microcline assemblage and the quartz-dominated veins are cut by late, <0.5 mm muscovite veinlets.

When crushed and separated, this sample yielded oscillatory-zoned euhedral zircon (Fig. 5f) with generally high U contents (181-2452 ppm, typically 750-1500 ppm). There is lead loss evident in analyses of the zircons, presumably due to the relatively high U content of these grains, with ten analyses having gnerally high common Pb and lower ages (O3.1, O4.1, O6.1, O14.1, O18.1, O19.1, O22.1, O24.1, O24.2 and O25.1) than the main population of 17 analyses, which has a weighted mean $^{206}Pb/^{238}U$ age of 603.2 ± 3.8 Ma (MSWD = 1.3; Fig. 6f).

Titanite was separated from the O'Callaghans Granite in order to provide a cross-check on the age of the intrusion using multigrain TIMS dating. Five fractions, each comprising 20 grains (Fig. 8) were dated, forming a group of analyses with a spread beyond analytical uncertainty (Fig. 9). Three of the five analyses have equal $^{206}Pb/^{238}U$ within analytical uncertainty and yield a weighted mean age of 606.6 ± 1.0 Ma (MSWD = 0.13), which is interpreted as the emplacement age of the granite. This age, although slightly older than the 603.2 ± 3.8 Ma zircon age is indistinguishable within analytical uncertainty.

Textural evidence from thin section suggests that the paragenesis of titanite is complex. Some appears to be part of the primary magmatic assemblage, but some appears to be associated with hydrothermal microcline. Partial isotopic resetting during alteration may account for the spread beyond analytical uncertainty of the titanite TIMS data.

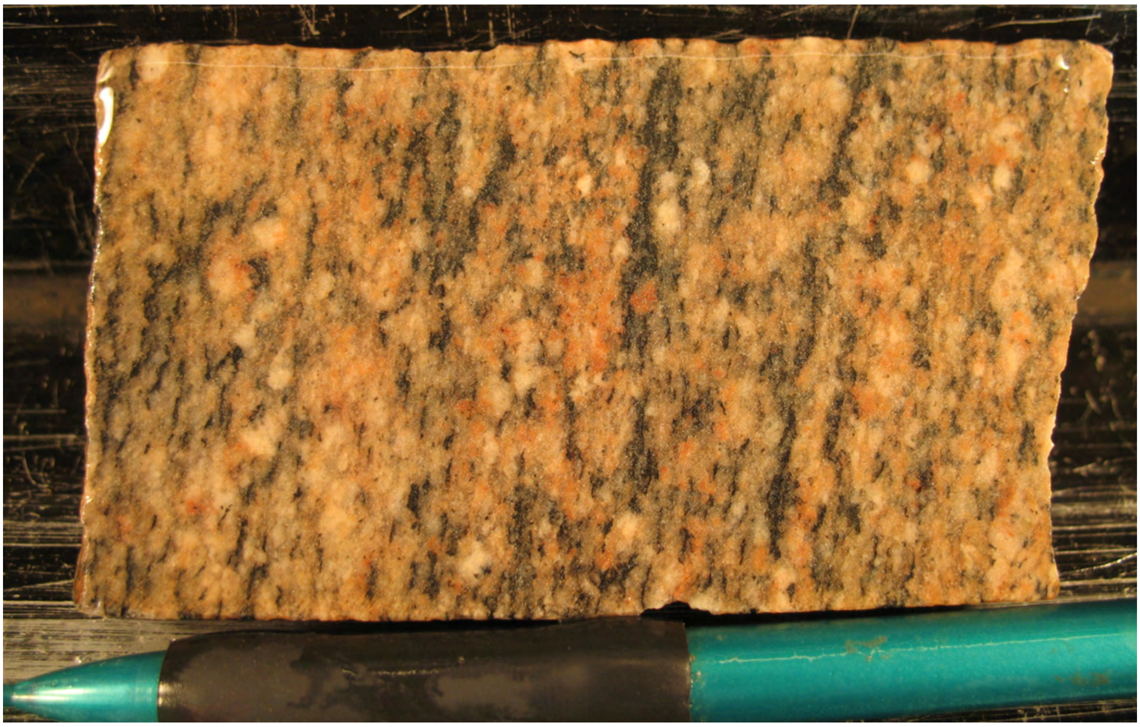

Fig. 7. *Foliation defined by oriented biotite and feldspar in the O'Callaghans Granite.*

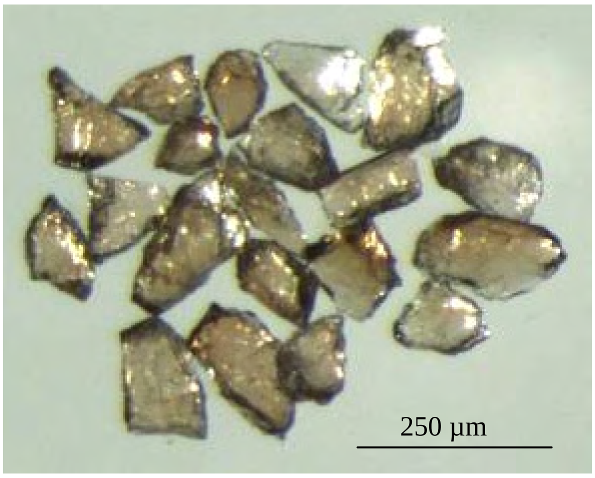

Fig. 8. *Titanite fraction from the O'Callaghans Granite..*

SUMMARY OF GRANITE AGES

A summary of granite ages obtained in this study is presented in Table 1, which includes SHRIMP U-Pb titanite ages obtained by Dunphy and McNaughton (1998) for the Mount Crofton Granite, which was not able to be dated in this study. Dunphy and McNaughton (1998) noted that U-Pb zircon ages previously obtained for granites in the region were typically younger than titanite ages from the same intrusives, and suggested that this was a result of Pb loss from high-U grains, with the titanite ages yielding the most reliable ages for magmatism. The indistinguishable SHRIMP zircon and TIMS titanite ages for the O'Callaghans Granite, indicate that the zircon dating can yield coherent ages for these intrusives by targeting analyses using CL imagery, which was unavailable to earlier workers.

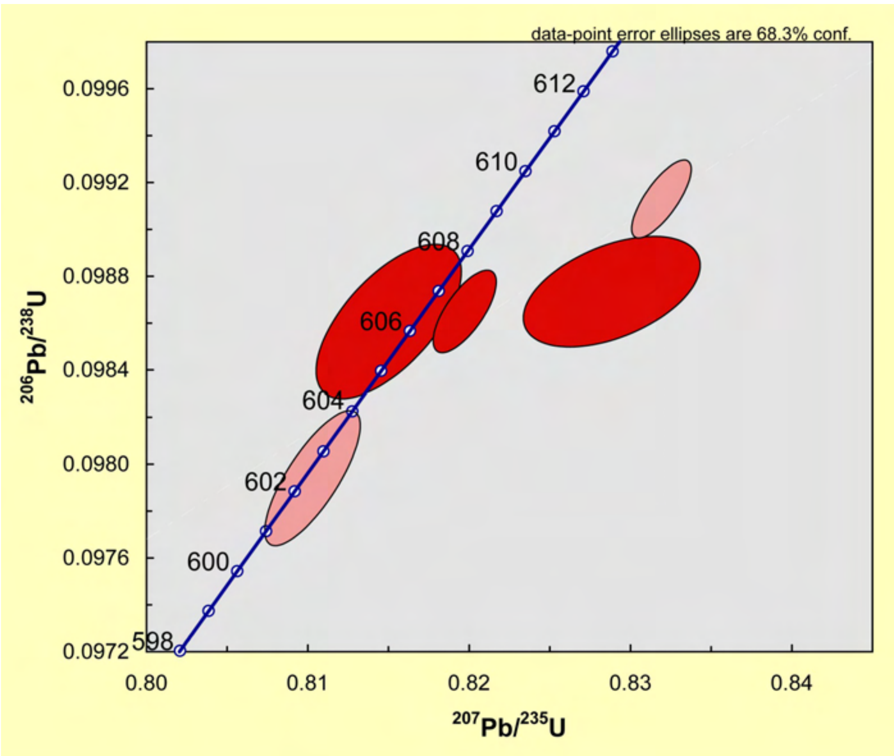

Fig. 9. *Concordia plot of titanite TIMS analyses from the O'Callaghans Granite.*

The granite ages obtained show no obvious correlation with oxidation state or magnetic susceptibility, and it is possible that the variable oxidation state of the Paterson granites is related to the oxidation state of the rocks they intrude, rather than being a primary igneous feature (Budd et al., 2001).

The ages obtained appear to show a degree of clustering, with four granites having ages of ~645 Ma, two with ages of ~630 Ma and one at ~605 Ma. Felsic magmatism thus appears to have been episodic, spanning a period of approximately 40 million years and a consequence of the Miles Orogeny. A significant amount of deformation evidently took place prior to ~645 Ma, when the Crofton Granite cross-cut NW-trending folding to the north of Telfer. The strong mineral foliation in the O'Callaghans Granite indicates that deformation extended until at least ~605 Ma.

Table 1: Summary of granite ages from the Paterson Province

GRANITE	**AGE (Ma)**
Wilki Granite	645 ± 4
Unnamed granite, Prefect Prospect	645 ± 4
Unnamed granite, NW of Minyari	644 ± 4
Minyari Granite	630 ± 4
Unnamed granite, ENE of Telfer	628 ± 4
O'Callaghans Granite	603 ± 4 (zircon), 607 ± 1 (titanite)
Crofton Granite	640 ± 8, 654 ± 8 (titanite)*

*Data from Dunphy and McNaughton (1998).

Dating of mineralisation

Several samples of reef and vein mineralisation were provided by Newcrest to constrain the timing of the main mineralising events at Telfer (Fig. 10). Two samples of the early quartz reefs (Middle Vale Reef and B30 Reef), one sample of a discordant North-Dipping Vein (Oakover) and one of a discordant Northwest-striking vein (NWV) were sampled to bracket the main mineralising events. Samples weighing several kilograms were taken from underground exposures, with care taken not to include wall rocks. Results are tabulated in Appendix 2.

MIDDLE VALE REEF (NEWCREST SAMPLE 8), GA SAMPLE 2007670009

Sample 2007670009 consists of a brecciated quartz veins with supergene chalcocite largely forming a matrix to quartz fragments (Fig. 11). The brecciated quartz is strongly undulose with extensive sub-grain development suggesting recrystallisation under strain. However, the infill to the breccia contains unstrained, clear and euhedral, growth-zoned quartz crystals that overgrow the strained quartz, and microplumose quartz infills the clear quartz (Fig. 12). This latter quartz type may be a product of recrystallisation of chalcedony (Morrison et al., 1990). Although it is possible that this quartz formed late during mineralisation, it is more likely the product of weathering.

The dominant sulphide mineral is chalcocite, which is present as infill between quartz breccia fragments. It comprises ~30% of the section examined. This mineral is interpreted to be a supergene mineral that has replaced mostly chalcopyrite. Hypogene chalcopyrite forms about 3% of the section and is present as remnant pools within chalcocite and in unreplaced veins in strained quartz. Pyrite, which also comprises ~3% of the section, is also present as anhedral to euhedral grains that are generally surrounded by chalcocite. This mineral is commonly associated with euhedral quartz and overgrown by microplumose quartz (Fig. 12). Other trace minerals present in the section include supergene bornite and covellite, which replace and vein chalcopyrite and high fineness gold that is present along fractures or on grain boundaries of strained quartz. Monazite and xenotime were not observed in the section examined, so their textural and genetic relationship to mineralisation is uncertain.

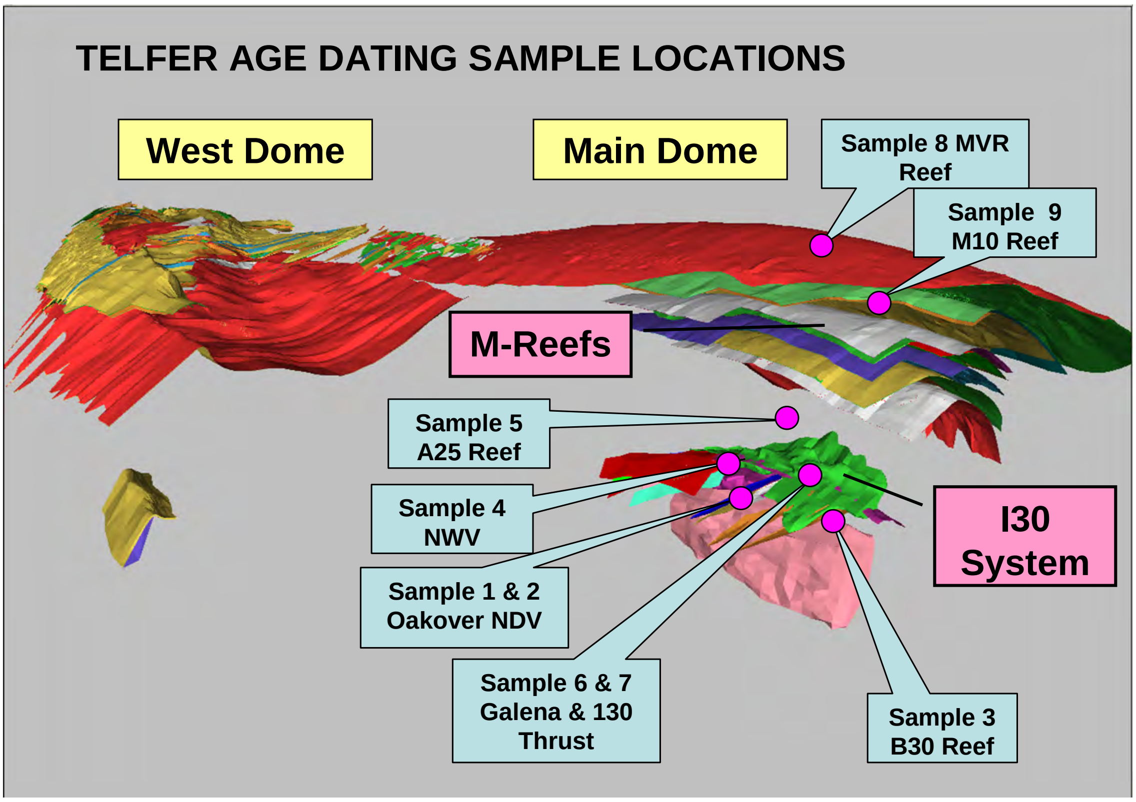

Fig. 10. *Locations of Telfer age dating samples, projected onto a 3-dimensional perspective view of reefs and veins. View to north.*

Four fractions of monazite and one fraction of xenotime were analysed from the Middle Vale Reef. All four monazite fractions are significantly discordant and do not constrain an accurate age for mineralisation (Fig. 13). The xenotime fraction is slightly reversely discordant, and yields a $^{207}Pb/^{235}U$ age of 628.2 ± 1.6 Ma (2σ). Given the evidence of isotopic complexity in this sample, and the slightly reversely discordant nature of the xenotime fraction, the 628.2 ± 1.6 Ma age is considered to represent a minimum age for mineralisation.

B30 REEF (NEWCREST SAMPLE 3), GA SAMPLE 2007670004

Two sections of sample 2007670004, from the B30 reef (Fig. 14), were examined, one sulphide-poor and one sulphide-rich. Both sections were dominated by anhedral, weakly to moderately undulose quartz with some sub-grain development. The sulphide-poor section contained accessory albite (3%) and dolomite (3%) that form discrete pools within quartz. The albite is dusted by muscovite and dolomite. With the exception of chalcopyrite, which forms pools within the quartz, other minor to trace minerals are closely associated with each other in the albite-dolomite pools. These include rutile, apatite, zircon, and xenotime. Zircon occurs as highly corroded grains (Fig. 15a), some of which have been partly recrystallised (Fig. 15b). In contrast, the xenotime is present as subhedral to euhedral grains to 100 µm (Fig. 15c), commonly with well developed growth zones (Fig. 15d). These relationships are interpreted to indicate that xenotime grew as part of the ore assemblage.

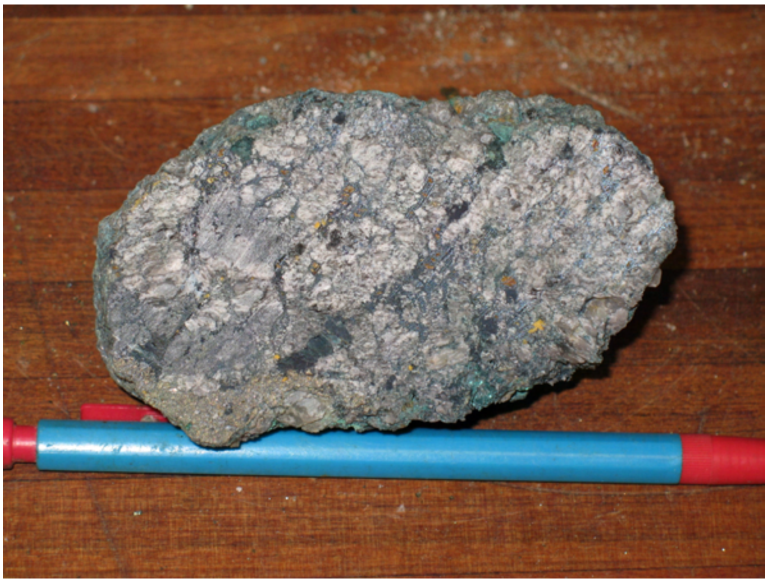

Fig. 11. *Sample of brecciated vein quartz from the Middle Vale Reef (2007670009). The dark grey mineral is chalcocite.*

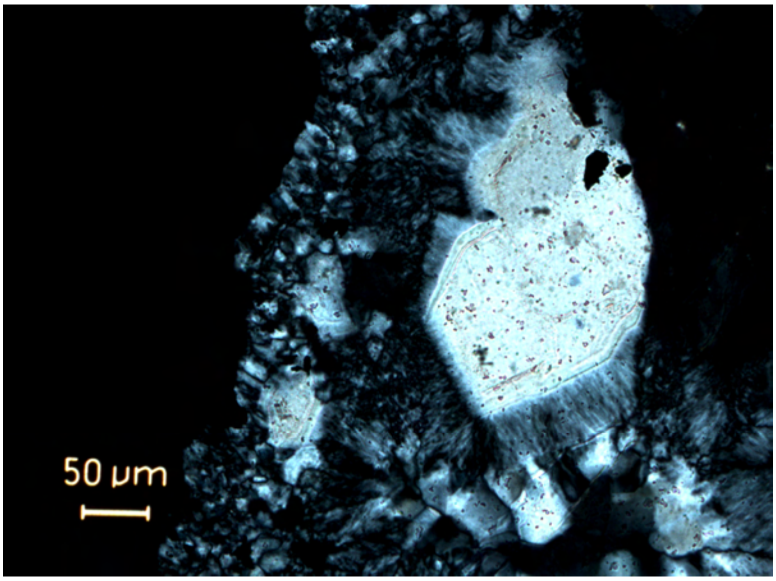

Fig. 12. *Photomicrograph from sample 2007670009 showing microplumose quartz overgrowing euhedral quartz. The opaque mineral is chalcocite.*

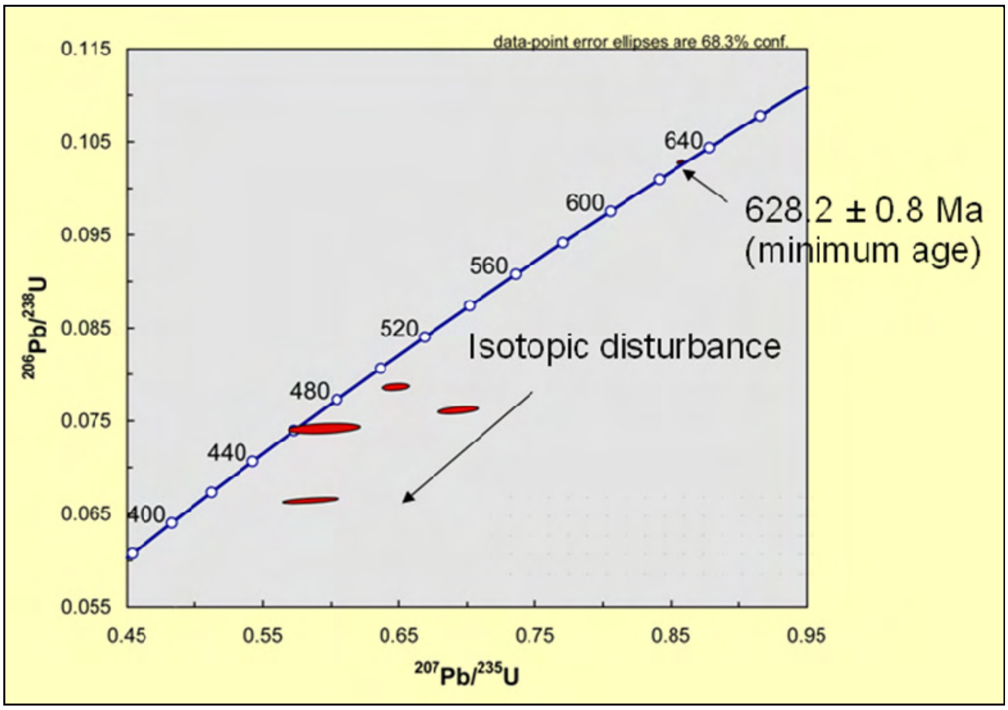

Fig. 13. Concordia plot of monazite and xenotime from the Middle Vale Reef. Age is at 1σ confidence level.

In contrast, the sulphide-rich section has up to 15% pyrite with accessory dolomite (2%) and minor to trace muscovite, chalcopyrite and rutile. As with the sulphide-poor section, the dolomite forms pools in association with muscovite and rutile. Pyrite is present as anhedral, fractured grains intergrown with quartz. Chalcopyrite occurs in fractures within the pyrite.

***Fig. 14.** Underground exposure quartz-pyrite veins of the B30 Reef.*

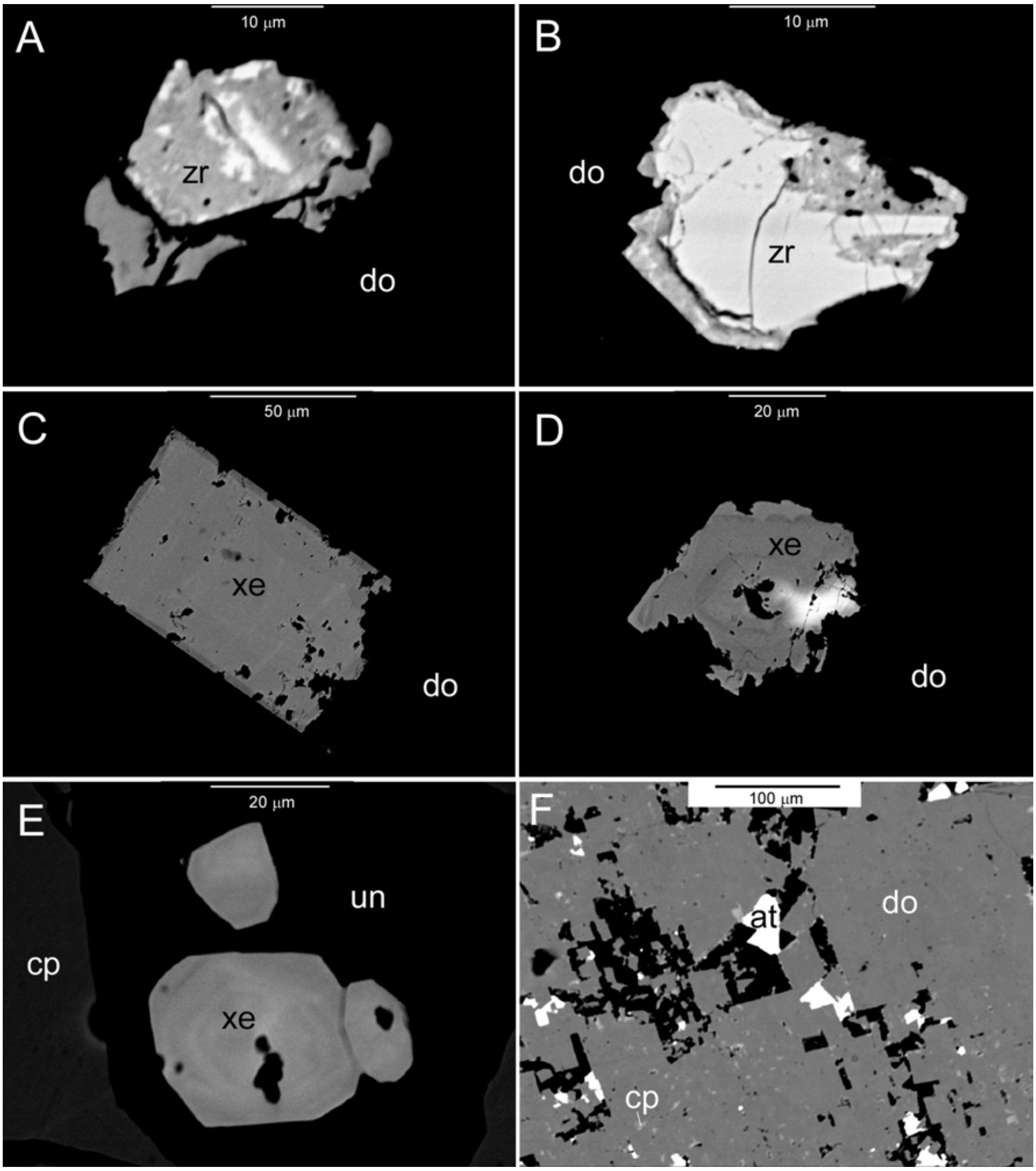

Fig. 15. *Scanning electron backscatter photomicrographs showing minerals and textures from samples 2007670004 (a-d) and 2007670002 (e-f): (a) corroded zircon (zr) grain in dolomite (do); (b) corroded and partly recrystallised zircon grain in dolomite; (c) euhderal xenotime (xe) grain with narrow dark rim in dolomite; (d) zoned euhedral xenotime grain in dolomite; (e) euhdral, zoned xenotime grain with unknown (un) as inclusion in chalcopyrite (cp); and (f) atacamite (at) grains associated with dolomite and chalcopyrite.*

Five fractions of xenotime and one fraction of monazite were analysed from a sample of the B30 Reef. Of the xenotime fractions, one is highly discordant and four others are near-concordant (Fig. 16). Of the near-concordant fractions, three are reversely discordant and little confidence can be placed in their inferred ages. One fraction showed evidence of minor isotopic disturbance, yielding a $^{207Pb}Pb/^{206}Pb$ age of 640.3 ± 3.4 Ma (2σ), which is interpreted as a minimum age for mineralisatsion. The monazite fraction is near-concordant, yielding a $^{207}Pb/^{206}Pb$ age of 652.2 ± 7.2 Ma (2σ), and is interpreted to represent the best estimate of the timing of mineralisation for the B30 reef.

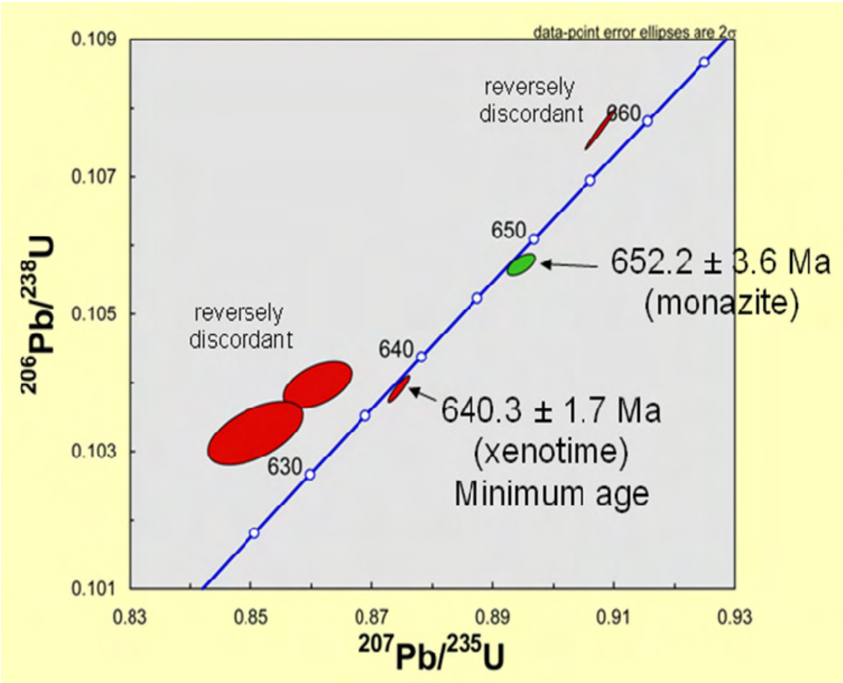

Fig. 16. *Concordia plots of monazite and xenotime from sample 2007670004, B30 Reef.*

OAKOVER NORTH-DIPPING VEIN (NEWCREST SAMPLE 1), GA SAMPLE 2007670002

Sample 2007670002 (Fig. 17) comes from a massive dolomite-chalcopyrite vein that forms part of the Oakover vein system (Fig. 18). The section examined contained ~80% calcite and 15-20% chalcopyrite. Accessory (2%) pyrite is also present, along with trace sphalerite, bornite, atacamite, xenotime and an unidentified mineral. Textural relationships suggest the following paragenesis: early, fine-grained dolomite → coarser-grained dolomite-chalcopyrite-pyrite-sphalerite-bornite-unidentified mineral-xenotime → late dolomite-atacamite-chalcopyrite. Most (>95%) of the section is part of the intermediate paragenetic assemblage, with the early and late assemblages minor. In the intermediate assemblage, dolomite, chalcopyrite, pyrite and sphalerite are intergrown, and bornite is present along growth zones in pyrite. Xenotime is present as 10-30 µm, zoned, subhedral to euhedral grains intergrown with the unidentified mineral as inclusions in chalcopyrite (Fig. 15e). Qualitative EDS analyses on the SEM indicate that the unidentified mineral is dominated by Ca and Cl. The early dolomite is present as 50-200 µm subhedral to euhedral grains included in the later coarser-grained dolomite. The last paragenetic assemblage consists of open-space-filling Fe-Mg-bearing calcite with atacamite and chalcopyrite filling voids within the coarser-grained dolomite (Fig. 15f).

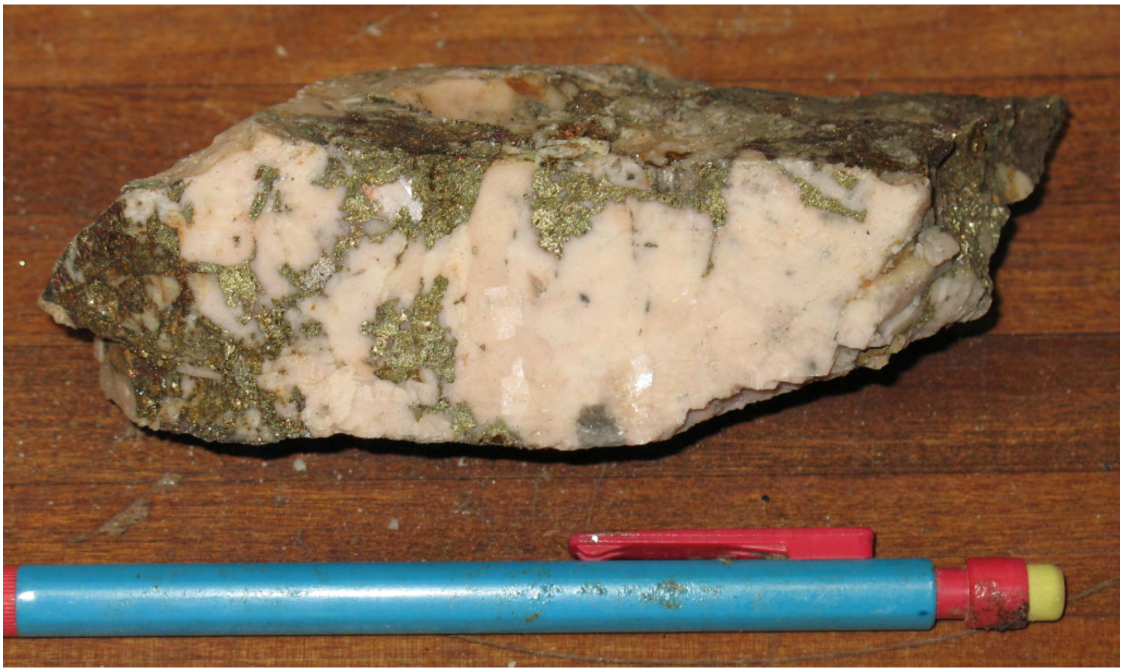

Fig. 17. *Hand specimen of the Oakover north-dipping dolomite-chalcopyrite vein (sample 2007670002).*

Four fractions of xenotime were analysed from this sample (Fig. 19). One fraction is reversely discordant with large analytical uncertainties, while the remaining three fractions are significantly discordant, yielding ^{207Pb}Pb/^{206}Pb ages of ca. 477, 562 and 623 Ma. The large degree of isotopic disturbance in this sample means that the ages obtained from these fractions have a large degree of uncertainty, and a robust age for mineralisation cannot be established from these data.

NORTHWEST-TRENDING VEINS (NEWCREST SAMPLE 4), GA SAMPLE 2007670005

Sample 2007670005 (Fig. 20) consists of very coarse-grained dolomite-quartz-chalcopyrite vein rock, with about 50% dolomite 30% quartz and 15-20% chalcopyrite. The section also contains accessory marcasite (3%), and trace sphalerite, pyrrhotite, pyrite, galena, cubanite (?), xenotime (?), and covellite. The sulphide minerals generally form pools or coarse aggregates within the dolomite. Chalcopyrite commonly has 50-100 μm rims of birds-eye textured marcasite. These marcasite rims, in some cases, are overgrown by 10-30 μm pyrite rims. Marcasite is also present as polycrystalline pools with inclusions of sphalerite and pyrrhotite. The marcasite is interpreted as a supergene alteration product of pyrrhotite. Sphalerite also is present as inclusions in chalcopyrite; in one occurrence the sphalerite is accompanied by galena. In another instance, sphalerite is associated with possible cubanite and a 5 μm grain of xenotime.

Fig. 18. *Underground exposure of the Oakover north-dipping dolomite-chalcopyrite vein.*

Data from five fractions of xenotime are plotted in Figure 21. The analyses range from near-concordant to highly discordant, with the least discordant fraction having a $^{207}Pb/^{206}Pb$ age of 642.0 ± 5.2 Ma (2σ). The data points form a well-defined linear array with an upper intercept age of 644.7 ± 7.1 Ma, a lower intercept age of 51 ± 13 Ma and an MSWD of 1.09. The data array is consistent with varying degrees of relatively recent resetting of a single population with an age of c. 645 Ma..

DOLOMITE-GALENA VEIN (NEWCREST SAMPLE 6), GA SAMPLE 2007670007

Sample 2007670007 consists of dolomite-galena vein rock with three paragenetic stages: coarse-grained euhedral dolomite → fine-grained anhedral dolomite-galena → fine-grained, anhedral to botryoidal dolomite. The first stage also contains minor chalcopyrite along growth zones in dolomite, and minor to trace bornite, chalcopyrite, which replaces the bornite, and pyrite are associated with dolomite and to a lesser extent galena in the intermediate paragenetic stage. The last stage is interpreted as supergene.

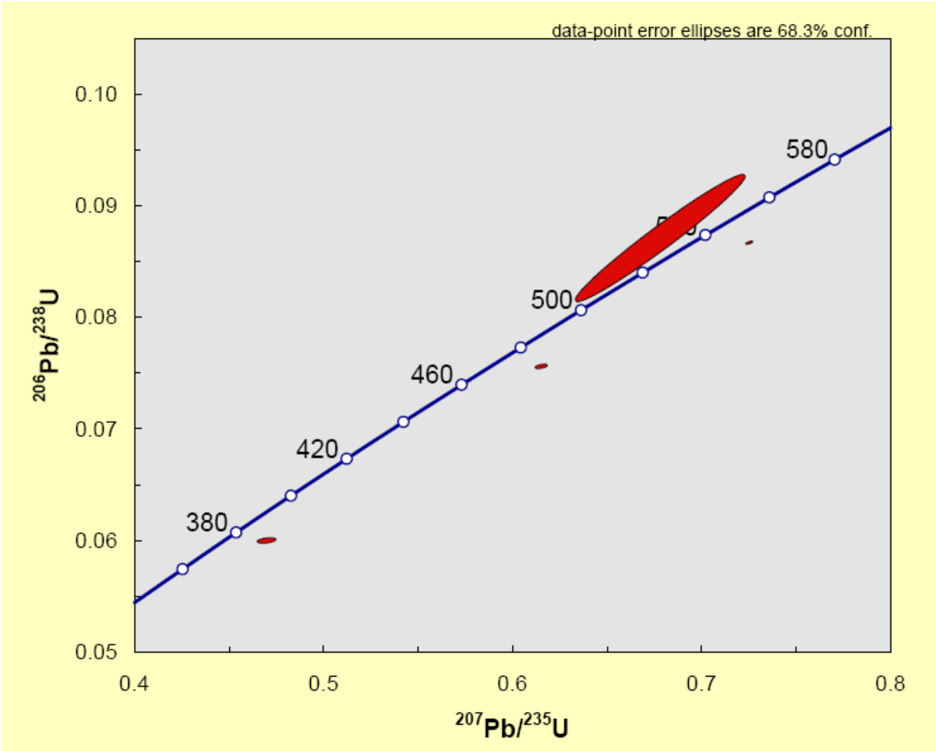

Fig. 19. *Concordia plot of xenotime U-Pb data from the Oakover north-dipping vein.*

Fig. 20. *Sample of northwest-trending dolomite-quartz-chalcopyrite vein .*

Lead isotope analysis of the galena yielded $^{206}Pb/^{204}Pb$, $^{207}Pb/^{204}Pb$ and $^{208}Pb/^{204}Pb$ ratios of 18.613, 15.797, and 38.932, respectively. Figure 22 plots this analysis against publicly available analyses of galena mineral deposits in the Yeneena Basin. It is significantly more radiogenic than Nifty and Warrabarty galena analyses, and also existing least radiogenic analyses of galena from veins in the hanging wall to the Middle Vale Reef (Goellnicht et al., 1989). It is isotopically most similar to the well-defined grouping of analyses from the O'Callaghans deposit, the significance of which is unclear.

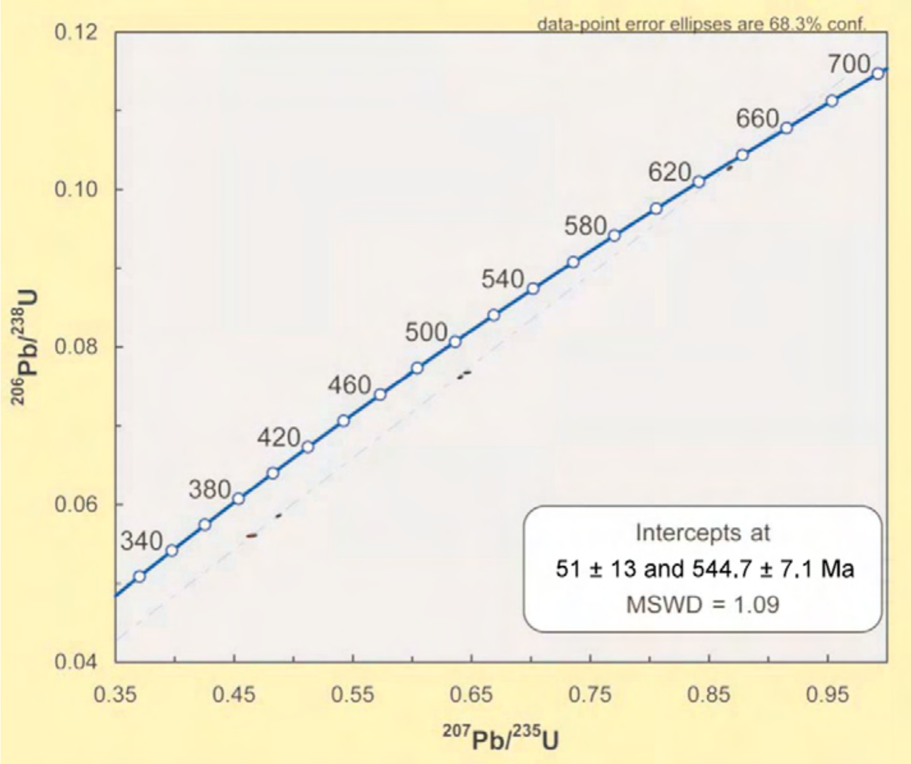

Figure 21. *Concordia plot of xenotime U-Pb data from a Northwest-trending vein.*

Relationship between granites and mineralisation

Although isotopic disturbance makes it difficult to define precise ages for some vein sets, the data provide sufficient information to establish the temporal relationship between granite emplacement and Au mineralisation. A summary of the U-Pb age data is presented below and in Table 2.

Cross-cutting relationships indicate that the concordant Middle Vale Reef and the B30 Reef are part of the earliest-formed Au-bearing vein sets in the Telfer deposit, with the isotopic data indicating an emplacement age of 652 ± 7 Ma. The 645 ± 7 Ma age obtained for the discordant NWV vein, which was emplaced at a relatively late stage, is indistinguishable within analytical uncertainty from that obtained from the early reef veins, indicating that mineralisation occurred over a relatively restricted period of time. The dating indicates that mineralisation at Telfer formed at a similar time to the emplacement of the earliest granite suite in the Paterson Province at ~645 Ma, and is not related to later granite intrusion at ~630 Ma and ~605 Ma.

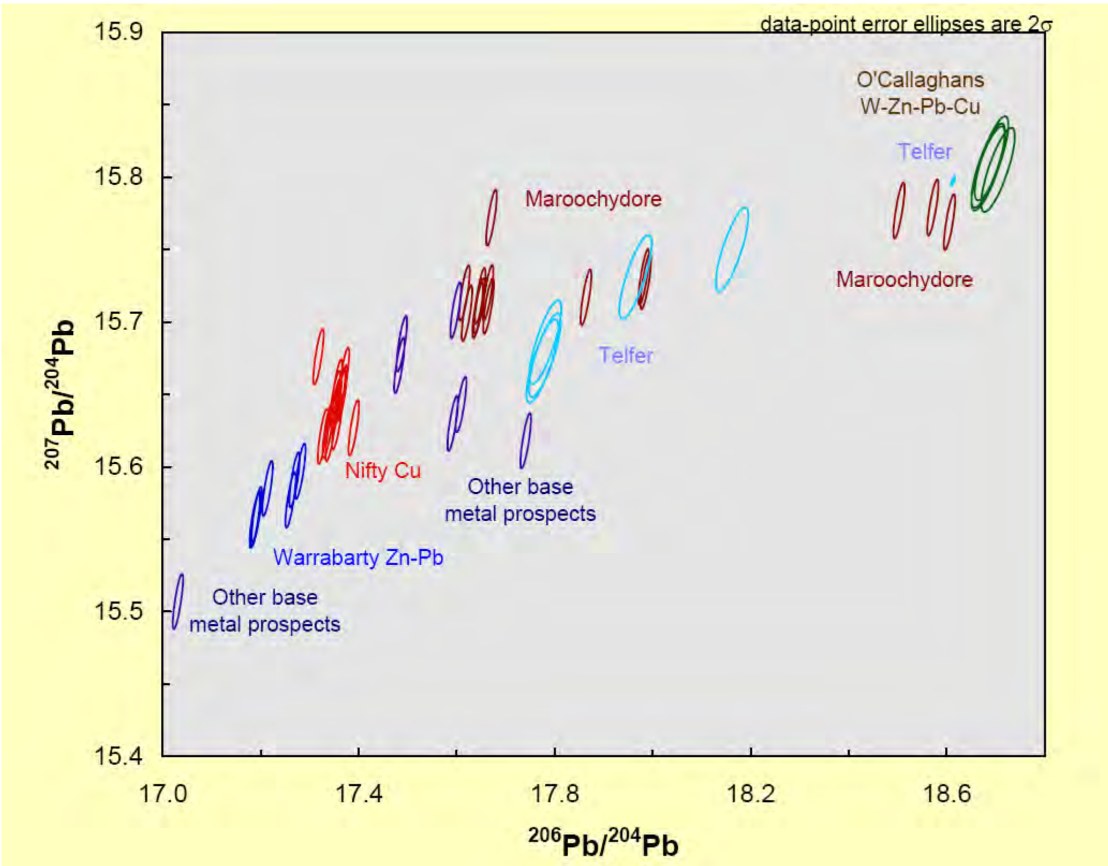

Fig. 22. *$^{206}Pb/^{204}Pb$ versus $^{207}Pb/^{204}Pb$ diagram showing the composition of galena and Pb-rich samples from various deposits in the Yeneena Basin. Published data are from Anderson (1999), Anderson et al. (2002), Froud (1997), Goellnicht et al. (1989), McKnight (1992), Reed (1996), and Smith (1996). The analysis from this study is the small ellipse(due to higher analytical precision) in the upper right of the diagram.*

Table 2: Summary age data for Au-bearing veins at the Telfer Mine

Vein	Interpreted age (Ma)
Middle Vale Reef	≥628.2 ± 1.6
B30 Reef	652.2 ± 7.2
Oakover NDV	≥623
NWV	644.7 ± 7.1

Although the timing constraints indicate that magmatism and Au mineralisation were coeval, they do not discriminate between opposing models that consider the granites to be either the dominant metal sources or heat sources that drove fluid scavenging of metals from the sedimentary succession. However, it is interesting to note that Au mineralisation probably did not take place during the later phases of granite emplacement and that the later granites are not geochemically distinct from the granites that were emplaced during mineralisation. This might indicate that granite emplacement *per se* was not a key factor in the formation of Au mineralisation, but was instead merely another expression of the tectonism that affected the Yeneena Basin (the Miles Orogeny). If this was the case, then the initial metamorphic dewatering of the Yeneena Supergroup during the Miles Orogeny might have been the major source of fluids and metals, with fluid flow and Au-deposition controlled by the syn-tectonic development of structural and chemical traps. This interpretation is perhaps supported by the fact that the Telfer deposit is not spatially associated with any known granite intrusion, with the nearest suitably-aged granite (the Wilki granite) being located ~10 km to the west, and the younger O'Callaghans Granite situated ~10 km to the SSE. If granites are not an essential component of the Au mineral system at Telfer, then it suggests that other parts of the Yeneena Basin lacking granite intrusions should not be considered unprospective based solely on the absence of felsic magmatism.

Conclusions

U-Pb SHRIMP Zircon and titanite dating of granites of the Paterson Province indicate that magmatism associated with the Miles Orogeny spanned the period 645-605 Ma. Although there are a limited number of ages currently available, these can be grouped into clusters at ~645, ~630 and ~605 Ma. Dating of xenotime and monazite from an early, concordant reef at the Telfer deposit indicates that mineralisation took place at 652 ± 7 Ma, while a late-stage discordant vein yields an age of 645 ± 7 Ma, indicating that Au mineralisation took place over a relatively restricted period of time. Gold-bearing veins at Telfer were thus emplaced at a similar time to the earliest granites associated with the Miles Orogeny, but the lack of a close spatial association between granite bodies and Au mineralisation at Telfer suggests that the granites might not have been an essential part of the mineral system.

Acknowledgements

Simon Bodorkos and Andrew Cross are thanked for comments on an early draft. James Maxlow and other Telfer geologists are thanked for providing samples and geological input.

References

Anderson, B. R., 1999. Structure, alteration and mineralisation of the Nifty copper deposit, Western Australia: implications for ore genesis. Unpublished Ph.D. thesis, University of Tasmania, 225pp.

Anderson, B. R., Gemmell, J. B and Nelson, D. R., 2002. Lead isotope evolution of mineral deposits in the Proterozoic Throssell Group, Western Australia. *Economic Geology,* **97,** 897-911.

Bagas, L., 2004. Proterozoic evolution of the northwest Paterson Orogen, Western Australia. *Precambrian Research,* **128,** 475–496.

Bagas, L. and Nelson, D. R., 2007. Provenance of Neoproterozoic sedimentary rocks in the northwest Paterson Orogen, Western Australia. *Northern Territory Geological Survey Special Publication,* **2.** (www.conferences.minerals.nt.gov.au/cabsproceedings/)

Bagas, L. and Smithies, R.H., 1998. Connaughton, W.A. Sheet 3452. *Geological Survey of Western Australia 1:100 000 Geological Series.*

Budd, A. R., Wyborn, L. A. I. and Bastrakova, I. V., 2001, The metallogenic potential of Australian Proterozoic granites: *Geoscience Australia Record,* **2001/12.**

Camacho, A., Compston, W., McCulloch, M. and McDougall, I. 1997. Timing and exhumation of eclogite facies shear zones, Musgrave Block, central Australia. *Journal of Metamorphic Geology,* **15,** 735-751.

Chin, R. J., Hickman, A. H. and Towner, R. R. 1982. Paterson Range, W.A. (2nd edition) Sheet SF-51-6. *Geological Survey of Western Australia 1:250 000 Geological Series.*

Claoué-Long, J. C., Compston, W., Roberts, J. and Fanning, C. M., 1995. Two Carboniferous ages: a comparison of SHRIMP zircon dating with conventional zircon ages and $^{40}Ar/^{39}Ar$ analysis. *SEPM Special Publication,* **54,** 3-21.

Czarnota, K., McIntyre, A., Maidment, D. and Neumann, N., 2007. Revised geodynamic framework for the Neoproterozoic Paterson Orogen. Proceedings of Deformation in the Desert, Alice Springs, 9-13 July 2007. Specialist Group in Tectonics and Structrual Geology, Geological Society of Australia, 37.

Czarnota, K., Gerner, E., Maidment, D. W., Meixner, A. J. and Bagas, L, 2009. Paterson area 1:250 000 scale solid geology interpretation and depth to basement model – explanatory notes. *Geoscience Australia Record,* **2009/16,** 37pp.

Dimo, G., 1990. Telfer gold deposits. *Australian Institute of Mining and Metallurgy Monograph,* **16,** 643-651.

Dunphy, J.M. and McNaughton, N.J., 1998. Geochronology of the Telfer granitoids: zircon and titanite U–Pb SHRIMP data. *Geological Society of Australia Abstracts,* **49,** 127.

Durocher, K. E., Kyser, T. K., Marlatt, J. and Hanly, A., 2003. New $^{40}Ar/^{39}Ar$ ages from the central Paterson Orogen Western Australia. *Australian Journal of Earth Sciences,* **50,** 601-610.

Froud, J., 1997. Mineralization and alteration of the Goosewhacker prospect, Western Australia. Unpublished B.Sc. Honours thesis, University of Tasmania, 116pp.

Goellnicht, N. M., 1987. Constraints on the timing and source of gold mineralization at Main Dome, Telfer, Western Australia. Unpublished B.Sc. Honours thesis, University of Western Australia, 98pp.

Goellnicht, N. M., 1992, Late Proterozoic fractionated granitioids and their role in the genesis of gold and base-metal mineralisation in the Telfer district, Western Australia. Unpublished Ph.D. thesis, University of Western Australia, 132pp.

Goellnicht, N. M., Groves, D. I., McNaughton, N. J. and Dimo, G., 1989. An epigenetic origin for the Telfer gold deposit. *Economic Geology Monograph,* **6,** 151-167.

Goellnicht, N. M., Groves, D. I. and McNaughton, N. J., 1991. Late Proterozoic fractionated granitoids of the mineralized Telfer area, Paterson Area, Western Australia. *Precambrian Research,* **51,** 375-391.

Grey, K., Hocking, R. M., Stevens, M. K., Bagas, L., Carlsen, G. M.., Irimies, F., Pirajno, F., Haines, P. W. and Apak, S. N., 2005. Lithostratigraphic nomenclature of the Officer Basin and correlative parts of the Paterson Orogen, Western Australia. *Geological Survey of Western Australia Report,* **93,** 89pp.

Heaman, L. M., Erdmer, P., and Owen, J. V., 2002. U–Pb geochronologic constraints on the crustal evolution of the Long Range Inlier, Newfoundland. Canadian Journal of Earth Sciences, 39, 845-865.

Hickman, A. H. and Bagas, L., 1999. Geological evolution of the Palaeoproterozoic Talbot Terrane and adjacent Meso and Neoproterozoic successions, Paterson Orogen, Western Australia. *Geological Survey of Western Australia Report,* **71,** 91pp.

Howard, G. R., Hansen, T., Moore, C., Moffitt, P. J., Inglis, R. J., Carlson, R. D., Kirchner, I., Coupland, D., Leary, S. and Tomsett, A., 2000. Current geological understanding of Telfer Mine. *Australian Institute of Mining and Metallurgy Publications Series,* **3,** 135-142.

Howard, G. R., Maxlow, J., Helm, S., Inglis, R., Carlson, R. and Hansen, T., 2005. Telfer gold-copper mine: 26 million ounces and growing. Proceedings of Newgengold 2005, Perth, November 28-29, p. 179-198.

Huston, D. L., Maas, R., and Czarnota, K., 2007. The age and genesis of the Nifty copper deposit: back to the future. Geoscience Australia Professional Opinion, 2007/03, 26pp.

Huston, D. L., Maas, R., Miggins, D., Maidment, D., Czarnota, K., Preiss, W. and Cassidy, K., 2009. Neoproterozoic mineralisation in Australia: timing and geodynamic setting. Smart science for exploration and mining, Proceeding of the 10th Biennial SGA Meeting of the Society for Geology Applied to Mineral Deposits, Townsville, Australia, 17-20 August 2009, 285-287.

Maidment, D. W., 2007. New timing constraints on the evolution of the Rudall Complex, Western Australia – implications for Proterozoic reconstructions. Proceedings of Deformation in the Desert, Alice Springs, 9-13 July 2007. Specialist Group in Tectonics and Structrual Geology, Geological Society of Australia, 32.

Maidment, D., Huston, D., Maas, R.., Czarnota, K., Neumann, N., McIntyre, A. and Bagas, L., 2008. The Nifty-Kintyre-Duke Cu-U-Pb-Zn mineralising events: links to the evolution of the Yeneena Basin, NW Paterson Orogen. *Geological Survey of Western Australia Record,* **2008/2,** 27-29.

McIntyre, A., Bagas, L., Cassidy, K., Czarnota, K., Neumann, N., Meixner, T. and Huston, D., 2005. Proterozoic geology of the northwest Paterson Orogen, Western Australia: prospectivity, possibilities, progress, and the Permian problem. Central Australian Basins Symposium Abstracts, Northern Territory Geological Survey, Darwin.

McKnight, R., 1992. Constraints of the origin of the Broadhurst stratabound Cu mineralization, with emphasis on stratigraphic setting and timing of mineralization. Unpublished B.Sc. Honours thesis, University of Western Australia, 81pp.

McNaughton, N. J. and Goellnicht, N. M., 1990. The age and radiothermal properties of the Mount Crofton Granite, Teller area, Western Australia. *Australian Journal of Earth Sciences,* **37,** 103-106.

Nelson, D. R., 1995. Compilation of SHRIMP U–Pb zircon geochronology data, 1994. *Geological Survey of Western Australia Record,* **1995/3,** 244pp.

Reed, A.. 1996. The structural, stratigraphic and temporal setting of the Maroochydore copper prospect, Paterson orogen, Western Australia. Unpublished Ph.D. thesis, University of Western Australia, 289pp.

Rowins, S. M., Groves, D. I., McNaughton, N. J., Palmer, M. R. and Eldridge, C. S. 1997. A reinterpretation of the role of granitoids in the genesis of Neoproterozoic gold mineralization in the Telfer Dome, Western Australia. *Economic Geology,* **92,** 133-160.

Sheppard, S., Rasmussen, B., Muhling, J. R., Farrell, T. R. and Fletcher, I. R., 2007. Grenvillian-aged orogenesis in the Palaeoproterozoic Gascoyne Complex, Western Australia: 1030-950 Ma reworking of the Proterozoic Capricorn Orogen. *Journal of Metamorphic Geology,* **25,** 477-494.

Smith, S.G., 1996, Geology and geochemistry of the Warrabarty carbonate-hosted Zn-Pb deposit, Paterson Orogen, Wetern Australia. Unpublished Ph.D. thesis, University of Tasmania, 162pp.

Steiger, R. H. and Jäger, J. E., 1977. Subcommission on geochronology: convention on the use of decay constants in geo- and cosmochronology. *Earth and Planetary Science Letters,* **36,** 359-362.

Trendall, A. F. 1974. The age of a granite near Mount Crofton, Paterson Range Sheet. *Western Australia Geological Survey Annual Report 1973*, 92-96.

Turner, C. C. 1982. The Telfer Gold Deposits, Western Australia. Stratigraphy, sedimentology and mineralisation of the Proterozoic Yeneena Group, Unpublished PhD thesis. University of New England, 296pp.

Tyrwhitt, D. S., 1979. Stratabound gold deposits of Proterozoic age at Telfer, Western Australia. Proceedings of the 85th Anuual Convention, Northwest Mining Convention, Spokane, Washington.

Tyrwhitt, D. S., 1985. Exploration, development and geology of the Telfer Gold Mine, Great Sandy Desert, Western Australia. Proceedings of First International Conference for Prospecting in Arid Areas, Rabat, Morocco. Institution of Mining and Metallurgy (London), 11-19.

White, A. J. R., Allen, C. M., Beams, S. D., Carr, P. F., Champion, D. C., Chappell, B. W., Wyborn, D. and Wyborn, L. A. I., 2001. Granite suties and supersuites of eastern Australia. Australian Journal of Earth Sciences, 48, 515-530.

Williams, I. S. and Claesson, S., 1987. Isotopic evidence for the provenance and Caledonian metamorphism of high grade paragneisses from the Seve Nappes, Scandinavian Caledonides. Ion microprobe zircon U-Th-Pb. *Contributions to Mineralogy and Petrology,* **97,** 205-217.

Appendix 1. Results of SHRIMP analyses, Paterson granite samples

Grain. area	$^{206}Pb_c$ (%)	U (ppm)	Th (ppm)	$^{232}Th/^{238}U$	$^{206}Pb^*/^{238}U$	± (%)	$^{207}Pb^*/^{206}Pb^*$	± (%)	^{206}Pb-^{238}U Age (Ma)	± (1)
Minyari Granite (sample 2006671025)										
Magmatic zircons										
M1.1	0.25	82	47	0.60	0.1015	2.0	0.0587	3.6	623.3	12.1
M2.1	1.08	171	114	0.69	0.0989	1.9	0.0614	2.1	608.2	11.2
M4.1	0.21	181	168	0.96	0.1018	1.4	0.0600	1.5	625.2	8.3
M3.1	0.00	273	216	0.82	0.1013	1.3	0.0609	1.1	622.3	8.0
M5.1	0.05	1052	697	0.68	0.1030	1.4	0.0605	0.7	631.7	8.2
M6.1	0.16	98	71	0.74	0.1050	1.5	0.0589	2.2	643.9	9.2
M7.1	0.10	307	141	0.48	0.1045	1.4	0.0621	0.9	640.7	8.2
M8.1	0.01	111	73	0.68	0.1040	1.5	0.0603	2.3	637.8	9.0
M9.1	0.05	230	152	0.68	0.1025	1.4	0.0592	1.3	629.3	8.2
M10.1	0.15	159	134	0.87	0.1031	1.4	0.0613	1.9	632.4	8.6
M11.1	-0.05	520	626	1.25	0.1033	1.3	0.0601	0.8	633.9	7.9
M12.1	1.15	96	65	0.69	0.1015	1.5	0.0562	5.7	623.1	9.0
M15.1	0.06	179	126	0.73	0.1022	0.9	0.0604	1.6	627.0	5.6
M17.1	0.15	98	65	0.69	0.1017	1.1	0.0589	1.9	624.1	6.6
M18.1	0.18	212	151	0.74	0.1020	0.9	0.0613	1.3	626.3	5.4
M19.1	0.06	1104	627	0.59	0.1017	0.7	0.0609	0.5	624.3	4.3
M20.1	0.15	339	235	0.72	0.1028	0.8	0.0609	1.5	630.9	5.0
M22.1	0.00	173	166	0.99	0.1038	1.0	0.0610	1.3	636.7	5.8
M23.1	-0.03	562	440	0.81	0.1029	0.8	0.0602	0.8	631.2	4.6
Rejected analyses										
M16.1	-0.01	100	66	0.68	0.1066	1.1	0.0572	3.9	652.9	6.8
M21.1	-0.14	427	300	0.73	0.2274	0.8	0.0837	0.5	1320.7	9.7
Wilki Granite (sample 2005671291)										
Magmatic zircons										
W1.1	-0.06	201	194	1.00	0.1057	1.9	0.0607	1.2	647.6	11.8
W2.1	0.21	174	175	1.04	0.1030	1.9	0.0620	1.4	632.2	11.7
W-3.1	0.09	590	788	1.38	0.1023	1.9	0.0605	0.9	627.9	11.1
W4.1	0.12	479	431	0.93	0.1068	1.9	0.0612	1.0	654.1	11.7
W7.1	0.01	397	426	1.11	0.1052	1.3	0.0608	1.2	644.9	8.3
W9.1	-0.02	358	328	0.94	0.1066	1.3	0.0611	1.0	653.2	8.2
W10.1	-0.06	332	410	1.28	0.1056	1.3	0.0597	1.3	647.3	8.2
W11.1	-0.05	536	447	0.86	0.1042	1.3	0.0609	0.7	639.0	7.9
W12.1	-0.05	326	316	1.00	0.1055	1.3	0.0603	1.1	646.6	8.2
W13.1	0.09	313	363	1.20	0.1027	1.3	0.0604	1.0	630.3	8.0
W14.1	0.03	243	285	1.21	0.1049	1.4	0.0604	1.5	642.9	8.4
W15.1	0.07	268	286	1.11	0.1061	1.4	0.0623	1.0	650.1	8.4
W17.1	0.08	183	201	1.14	0.1053	0.9	0.0603	1.3	645.1	5.7
W19.1	0.02	420	436	1.07	0.1065	0.9	0.0620	0.8	652.4	5.3
W20.1	0.07	230	182	0.82	0.1064	0.9	0.0610	1.4	651.5	5.6
W21.1	0.06	316	384	1.26	0.1058	0.8	0.0611	1.0	648.1	5.2
W22.1	0.07	159	208	1.36	0.1026	1.0	0.0582	2.0	629.4	5.8

W24.1	0.02	263	384	1.51	0.1054	0.9	0.0599	1.1	646.2	5.3
W25.1	-0.02	289	338	1.21	0.1064	0.9	0.0618	1.2	651.9	5.3
Rejected analyses										
W5.1	0.25	574	664	1.20	0.1002	1.9	0.0608	1.0	615.5	11.1
W6.1	0.29	173	250	1.49	0.1009	2.0	0.0591	2.8	619.7	11.6
W8.1	1.50	211	202	0.99	0.0983	1.4	0.0595	4.0	604.6	7.9
W9.1	0.08	491	367	0.77	0.1771	1.3	0.0752	0.5	1051.3	12.9
W18.1	0.01	741	921	1.28	0.1077	0.8	0.0615	0.6	659.5	4.8
W23.1	0.23	246	257	1.08	0.1014	0.9	0.0614	1.7	622.6	5.4
Unnamed granite, Prefect prospect (sample 2006677122)										
Magmatic zircons										
P1.1	0.08	583	259	0.46	0.1025	1.9	0.0605	0.7	629.1	11.1
P2.1	0.09	589	177	0.31	0.1039	1.9	0.0615	1.0	637.1	11.3
P3.1	-0.09	304	74	0.25	0.1087	1.9	0.0592	1.1	665.0	12.0
P5.1	0.04	547	251	0.47	0.1044	1.9	0.0613	0.8	640.4	11.4
P6.1	-0.02	409	204	0.52	0.1064	1.9	0.0584	1.6	651.9	11.7
P7.1	0.14	727	181	0.26	0.1031	1.3	0.0615	0.7	632.3	7.7
P8.1	0.14	275	52	0.20	0.1051	1.3	0.0613	1.0	644.1	8.2
P9.1	0.02	489	181	0.38	0.1081	1.3	0.0612	0.9	661.5	8.4
P10.1	0.07	618	201	0.34	0.1035	1.3	0.0607	0.7	634.6	7.8
P11.1	0.01	220	161	0.76	0.1076	1.4	0.0617	1.1	659.1	8.7
P13.1	0.03	407	107	0.27	0.1036	1.3	0.0604	0.9	635.2	8.0
P14.1	0.16	168	104	0.64	0.1031	1.4	0.0622	1.2	632.6	8.5
P15.1	0.02	392	141	0.37	0.1059	1.3	0.0618	0.8	649.2	8.2
P17.1	0.01	362	85	0.24	0.1064	0.8	0.0622	1.1	651.7	5.1
P18.1	0.05	508	141	0.29	0.1070	0.8	0.0621	0.8	655.0	4.9
P19.1	0.42	367	112	0.32	0.1046	0.8	0.0632	1.0	641.4	5.2
P20.1	-0.02	327	122	0.38	0.1048	0.8	0.0613	1.0	642.7	5.1
P21.1	0.15	612	409	0.69	0.1052	0.8	0.0628	1.0	645.0	4.7
P22.1	0.11	263	167	0.65	0.1034	0.9	0.0617	1.1	634.2	5.2
P23.1	0.02	586	237	0.42	0.1050	0.8	0.0611	0.7	643.5	4.7
P24.1	-0.15	176	95	0.56	0.1054	0.9	0.0594	1.7	646.2	5.8
Rejected analyses										
P4.1	0.73	438	99	0.23	0.1262	1.9	0.0706	0.8	766.4	13.6
P12.1	0.26	194	379	2.02	0.1210	1.4	0.0667	1.0	736.2	9.7
P25.1	0.01	306	60	0.20	0.1077	0.8	0.0601	1.2	659.3	5.2
Unnamed granite, northwest of Minyari (sample 2006671004)										
Magmatic zircons										
U1.1	0.07	528	616	1.20	0.0995	1.9	0.0594	0.9	611.5	10.8
U2.1	0.06	575	160	0.29	0.1028	1.9	0.0602	0.8	630.9	11.3
U-3.1	0.22	341	385	1.17	0.0994	1.9	0.0616	1.0	611.1	11.0
U4.1	0.19	128	116	0.94	0.1032	2.0	0.0563	3.2	633.1	12.0
U5.1	0.15	394	394	1.03	0.1014	1.9	0.0607	1.3	622.6	11.3
U-6.1	0.10	585	598	1.06	0.1000	1.9	0.0600	1.1	614.4	11.0
U7.1	0.04	1897	2974	1.62	0.1008	1.3	0.0606	0.4	619.3	7.5
U9.1	0.07	856	947	1.14	0.1035	1.3	0.0613	0.6	635.1	7.9
U10.1	0.07	155	194	1.29	0.1016	1.4	0.0614	1.3	623.5	8.5
U11.1.1	0.01	226	147	0.67	0.1025	1.4	0.0582	1.5	629.3	8.2
U12.1	-0.04	336	99	0.30	0.1055	1.3	0.0610	1.1	646.4	8.2
U13.1	0.08	518	368	0.73	0.1014	1.3	0.0614	0.7	622.8	7.7
U16.1	0.10	254	211	0.86	0.1048	0.9	0.0627	1.0	642.4	5.4

U18.1	-0.07	179	213	1.23	0.1018	0.9	0.0578	1.9	624.9	5.6
U19.1	0.14	312	255	0.84	0.1017	0.8	0.0622	0.9	624.4	5.0
U20.1	0.05	244	167	0.71	0.1025	0.9	0.0609	1.6	629.0	5.3
U21.1	0.03	306	291	0.98	0.1030	0.8	0.0577	1.9	631.7	5.1
U22.1	0.19	221	115	0.54	0.1027	1.0	0.0604	1.4	630.2	6.2
U23.1	-0.06	738	380	0.53	0.1015	0.7	0.0597	0.6	623.3	4.4
U24.1	0.02	352	447	1.31	0.1031	0.8	0.0613	0.9	632.8	5.0
U25.1	-0.02	376	314	0.86	0.1016	0.8	0.0581	2.0	623.9	4.9
U26.1	-0.01	152	140	0.96	0.1032	1.0	0.0576	2.5	633.1	6.0
Rejected analyses										
U8.1	1.78	380	345	0.94	0.0948	1.3	0.0614	2.7	584.0	7.3
U14.1	-0.03	542	480	0.91	0.1066	1.3	0.0614	0.7	652.7	8.1
U17.1	0.23	320	392	1.26	0.1067	0.8	0.0612	1.7	653.4	5.2
Unnamed granite, east-northeast of Minyari Granite (sample 2005671325)										
Magmatic zircons										
N1.1	0.02	297	150	0.52	0.1061	1.9	0.0614	1.1	650.0	11.7
N2.1	0.24	180	104	0.60	0.1035	1.9	0.0630	1.2	634.7	11.7
N3.1	0.10	373	152	0.42	0.1036	1.9	0.0604	1.2	635.5	11.4
N7.1	0.10	678	738	1.13	0.1036	1.3	0.0611	1.1	635.2	7.8
N8.1	0.16	130	70	0.56	0.1037	1.4	0.0601	3.4	636.2	8.8
N10.1	0.14	331	187	0.58	0.1032	1.3	0.0621	0.9	633.3	8.0
N11.1	0.01	272	217	0.83	0.1047	1.4	0.0605	1.1	641.9	8.3
N12.1	0.05	254	189	0.77	0.1055	1.4	0.0604	1.4	646.3	8.3
N13.1	0.72	276	162	0.61	0.1027	1.3	0.0605	2.3	630.4	8.1
N14.1	0.29	394	266	0.70	0.1043	1.3	0.0627	1.0	639.7	8.1
N15.1	0.11	227	170	0.78	0.1045	1.4	0.0594	1.5	640.8	8.4
N15.2	-0.02	223	172	0.79	0.1052	1.4	0.0608	1.6	645.1	8.5
N14.1	-0.14	470	365	0.80	0.1063	0.8	0.0596	0.8	651.0	4.9
N17.1	-0.02	261	141	0.56	0.1068	0.9	0.0613	1.0	653.9	5.4
N18.1	-0.13	212	124	0.60	0.1077	0.9	0.0587	1.6	659.4	5.7
N19.1	0.08	232	182	0.81	0.1059	0.9	0.0620	1.0	648.8	5.5
N20.1	0.22	145	71	0.51	0.1039	1.0	0.0578	3.0	637.2	6.1
N21.1	0.02	325	129	0.41	0.1044	0.8	0.0595	1.3	640.0	5.0
N23.1	0.18	273	189	0.72	0.1048	0.9	0.0607	1.8	642.7	5.2
N24.1	0.03	183	91	0.51	0.1057	1.0	0.0593	2.0	647.7	6.0
Rejected analyses										
N4.1	0.28	289	120	0.43	0.2712	2.0	0.0977	0.6	1546.9	27.7
N5.1	-0.01	229	156	0.70	0.1111	1.9	0.0591	2.3	679.0	12.5
N6.1	0.00	145	80	0.57	0.1088	2.0	0.0643	2.7	665.7	12.7
N22.1	0.17	248	128	0.53	0.2217	1.0	0.0853	0.8	1290.7	11.2
O'Callaghans Granite, northwest of Minyari (sample 2007670001)										
Magmatic zircons										
O1.1	0.05	1133	361	0.33	0.0989	1.8	0.0597	0.6	608.2	10.7
O2.1	0.26	1445	1032	0.74	0.0983	1.8	0.0599	0.7	604.4	10.6
O5.1	0.21	1545	870	0.58	0.0961	1.8	0.0601	0.7	591.3	10.4
O7.1	1.28	1424	836	0.61	0.0964	1.6	0.0611	1.7	593.5	9.2
O8.1	0.38	667	858	1.33	0.0983	1.4	0.0603	1.3	604.2	8.0
O9.1	0.22	915	284	0.32	0.0987	1.3	0.0596	1.0	606.7	7.4
O10.1	0.49	1163	532	0.47	0.0975	1.3	0.0595	1.1	600.0	7.6
O11.1	0.09	842	358	0.44	0.0977	1.3	0.0599	0.7	601.0	7.3
O12.1	0.11	1387	566	0.42	0.0986	1.3	0.0602	0.5	606.4	7.3

O13.1	0.09	1150	472	0.42	0.0972	1.3	0.0602	0.5	597.8	7.3
O15.1	0.15	1369	506	0.38	0.0964	1.3	0.0604	0.7	593.6	7.2
O17.1	0.01	1664	1258	0.78	0.0995	0.7	0.0602	0.4	611.2	4.2
O20.1	0.14	721	568	0.81	0.0974	0.9	0.0600	0.8	599.0	5.0
O23.1	0.16	1277	586	0.47	0.0962	0.7	0.0598	0.6	592.1	4.0
O26.1	0.04	2453	1612	0.68	0.0996	0.7	0.0603	0.4	612.3	4.1
O27.1	0.12	257	75	0.30	0.0985	0.9	0.0583	1.8	605.6	5.4
O28.1	0.40	181	238	1.36	0.0990	0.9	0.0599	2.5	608.8	5.5
Rejected analyses										
O3.1	0.94	2016	1216	0.62	0.0909	1.8	0.0603	1.1	560.7	9.9
O4.1	0.24	2156	1179	0.57	0.0940	1.8	0.0600	0.6	579.0	10.1
O6.1	1.97	1050	447	0.44	0.0942	1.8	0.0607	2.7	580.2	10.3
O14.1	0.09	962	537	0.58	0.0959	1.4	0.0590	0.8	590.6	8.2
O18.1	0.26	1543	939	0.63	0.0929	0.8	0.0601	0.7	572.5	4.1
O19.1	0.35	1386	663	0.49	0.0949	0.8	0.0604	0.9	584.7	4.4
O22.1	0.14	1259	658	0.54	0.0960	0.8	0.0604	0.6	591.1	4.5
O24.1	0.54	1121	746	0.69	0.0955	0.7	0.0595	1.4	588.2	4.1
O24.2	0.27	804	499	0.64	0.0961	0.8	0.0608	0.9	591.7	4.3
O25.1	0.89	725	299	0.43	0.0936	0.8	0.0606	1.5	576.5	4.1

1. $\%^{206}Pb_c$ indicates the proportion of common ^{206}Pb in the total measured ^{206}Pb.

2. Pb isotopic ratios corrected for common Pb by reference to the measured ^{204}Pb.

3. $^{206}Pb/^{238}U$ calculated using ^{207}Pb correction.

4. All errors quoted as 1σ.

Appendix 2. Results of ID-TIMS U-Pb analyses of titanite from O'Callaghans Granite and xenotime and monazite from mineralised veins from the Telfer deposit.

Mineral	Mass (mg)	U (ppm)	Th (ppm)	Pb (ppm)	Th/U	TCPg (pg)	$^{206}Pb/^{204}Pb$	$^{206}Pb/^{238}U$	$^{207}Pb/^{235}U$	$^{207}Pb/^{206}Pb$	$^{206}Pb/^{238}U$ age (Ma)	$^{207}Pb/^{235}U$ age (Ma)	$^{207}Pb/^{206}Pb$ age (Ma)	%Disc
2007670001														
titanite (14)	30.0	189	63	19	0.33	16	2281	0.09861±22	0.81509±296	0.05995±17	606.3±1.3	605.3±1.7	601.7±6.0	-0.8
titanite (19)	36.7	147	42	15	0.29	15	2277	0.09866±12	0.81980±129	0.06027±7	606.5±0.7	607.9±0.7	613.2±2.4	1.1
titanite (13)	15.9	128	36	13	0.28	7	1819	0.09874±16	0.82890±360	0.06088±23	607.0±0.9	613.0±2.0	635.2±8.2	4.6
titanite (17)	29.4	161	81	17	0.50	14	2070	0.09913±11	0.83199±122	0.06087±6	609.3±0.6	614.7±0.7	634.6±2.0	4.2
titanite (19)	30.4	198	54	20	0.27	19	1911	0.09795±19	0.81040±195	0.06001±9	602.4±1.1	602.7±1.1	603.8±3.3	0.3
2007670002														
xenotime (4)	15.8	634	1810	68	2.86	23	1662	0.06010±16	0.46927±325	0.05663±36	376.2±1.0	390.7±2.2	477.2±14.0	21.8
xenotime (4)	8.5	690	1570	93	2.28	4	8436	0.08681±10	0.72467±121	0.06054±8	536.6±0.6	553.4±0.7	623.0±2.7	14.4
xenotime (5)	16.8	676	869	67	1.29	28	1955	0.07571±13	0.61455±207	0.05887±17	470.5±0.8	486.4±1.3	562.4±6.4	16.9
xenotime (4)	6.7	214	2200	73	10.27	7	1185	0.08720±376	0.67764±2982	0.05636±55	539.0±22.3	525.3±17.9	466.6±21.5	-16.2
2007670004														
xenotime (5)	17.8	1072	611	79	0.57	7	11879	0.06770±8	0.56771±79	0.06081±4	422.3±0.5	456.5±0.5	632.7±1.4	34.4
xenotime (5)	33.0	775	468	90	0.60	7	26109	0.10770±25	0.90779±210	0.06113±2	659.4±1.4	655.9±1.1	643.9±0.8	-2.5
xenotime (6)	24.5	1018	494	113	0.48	48	3374	0.10399±28	0.86111±460	0.06006±28	637.7±1.6	630.7±2.5	605.7±10.0	-5.5
xenotime (4)	19.4	939	833	113	0.89	9	12995	0.10393±15	0.87453±144	0.06103±5	637.4±0.9	638.0±0.8	640.3±1.7	0.5
xenotime (3)	21.0	841	511	95	0.61	19	6156	0.10328±38	0.85092±640	0.05975±37	633.6±2.2	625.2±3.5	594.6±13.5	-6.9
monazite (1)	19.8	274	6899	228	25.18	8	4415	0.10573±13	0.89466±190	0.06137±10	647.9±0.7	648.9±1.0	652.2±3.6	0.7
2007670005														
xenotime (5)	14.6	447	410	31	0.92	8	2787	0.05630±9	0.46565±265	0.05998±31	353.1±0.6	388.2±1.8	602.9±11.1	42.6
xenotime (4)	6.0	446	147	36	0.33	10	1362	0.07698±9	0.64657±164	0.06092±14	478.1±0.6	506.4±1.0	636.3±4.8	25.8
xenotime (6)	23.0	537	716	43	1.33	8	5675	0.05882±14	0.48816±129	0.06019±11	368.5±0.9	403.7±0.9	610.3±3.8	40.8
xenotime (3)	10.9	596	978	64	1.64	4	8364	0.07646±9	0.64059±112	0.06077±8	474.9±0.5	502.7±0.7	631.0±2.8	25.7
xenotime (5)	27.3	390	282	45	0.72	7	9983	0.10289±13	0.86653±141	0.06108±7	631.3±0.8	633.7±0.8	642.0±2.6	1.8
2007670009														
xenotime (5)	5.4	160	4283	109	26.77	7	508	0.06660±20	0.58510±1365	0.06372±138	415.6±1.2	467.7±8.7	732.3±45.1	44.6
xenotime (5)	17.3	135	3300	87	24.53	55	227	0.07881±23	0.64706±663	0.05955±59	489.0±1.4	506.7±4.1	587.2±21.4	17.4
xenotime (5)	8.7	170	3790	100	22.33	79	105	0.07435±36	0.59493±1728	0.05803±162	462.3±2.2	474.0±10.9	531.0±60.0	13.4
xenotime (3)	40.6	140	2278	70	16.22	79	364	0.07630±26	0.69339±961	0.06591±83	474.0±1.5	534.8±5.7	803.5±26.3	42.5
xenotime (3)	12.3	578	496	69	0.86	6	7718	0.10298±14	0.85641±150	0.06032±8	631.8±0.8	628.2±0.8	614.9±2.9	-2.9

Notes: (1) Numbers in parentheses correspond to the number of crystals analysed; (2) atomic ratios corrected for blank (5pg Pb; 1pg U), fractionation and initial common Pb (Stacey and Kramers, 1975); (3) TCPb refers to the total amount of common lead present in the analyses in picograms; (4) Th concentration estimated from the amount of ^{208}Pb present in the analysis and the $^{207}Pb/^{206}Pb$ age; (5) %Disc refers to the amount of discordance along a reference line to zero age; and (6) all errors in this table are reported at 1 sigma (0.09402±2 means 0.09402±0.00002).